Greener Journal of Geology and Earth Sciences
ISSN: 2354-2268
Vol. 5(1), pp. 76-108, 2023

http://gjournals.org/GJGES

Highlighting the Fine Structure of the Seismic Zones of the Western Branch of the East African Rift System Using the Unified Characterization Scale and Its Geological Implication.

Mukange Besa Anscaire[1], Katwika Christian[3], Jalum Bill[1], Zana Ndotoni André[1], Tondozi Kento Franck [1, 2]

[1]Mention Physics, Faculty of Sciences and Technology, University of Kinshasa, Kinshasa, DR Congo.
[2]Departement of internal Geophysics, Center of Research in Geophysic (CRG), Kinshasa, DR Congo.
[3] Department of Mining, Polytechnic Faculty , University of Lubumbashi, Lubumbashi, DR Congo.

ARTICLE INFO

Article No.: *120423154*
***Type*:** *Research*
Full Text: *PDF, PHP, HTML, EPUB, MP3*

Accepted: *06/12/2023*
Published: *30/12/2023*

Corresponding Author
Prof. Mukange Besa Anscaire
E-mail: *anscairbesa@ yahoo.fr*

Keywords: *fine structure, East African rift, Congolese Rift, seismic species, characterization scale, heterogeneity rate, resemblance rate, fault location, d-value*

ABSTRACT

Previous research aimed at characterizing the seismicity of the DRC and its surroundings (Mukange, 2016; Mukange, 2021b) revealed that the seismic activity of the DRC is subdivided into two large zones: a non-rift zone (10°E -25°E) of low seismicity and a rift zone (25°E-35°E) of high seismicity; the average degree of heterogeneity of the region is 60%, with seismic activity concentrated in the main faults.

The main objective of this work is to highlight the fine structure of the Rift zones using the model which exploits the notion of seismic species and the precise location of the main underground faults by positing the hypothesis that: “the main faults are located in places where the module of seismic activity is at its peak”. We are interested in the rift zone (30°E-35°E. 6°N-14¨S). This zone includes the square grid zones A41, A42, A42, A44, A51, A52, A52 and A54 with a side of 5° each. The demonstration of their fine structure consists of subdividing them into squares of side 1° each by calculating certain parameters deduced from the fundamental seismic parameters covering the period from 1975 to 2013. This model, introducing new concepts, led to the results following, some of which go beyond the known: Regarding the fine structure, we note:

- that the rift zone (25-35°E), formerly homogeneous, is now subdivided into two distinct sub-zones:
- The area located between 25 and 30°E (A42, A43 and A44). However, we notethat the structure of zone A44 (Upemba rift zone in the upper Katanga region) straddles between A42T (Virunga-Lake Kivu zone) and A43T (Tanganyika zone).
- The zone between 30 and 35°E (A51, A52, A53 and A54). However, zones A42T (Kivu zone) and A54T (Malawi zone) have some similarities,
- The rate of resemblance between the two sub-zones is 25%: the first zone is less seismic than the second, one having a form factor (III), the other (IV),
- that the structure of the entire established DRC is almost identical to that of the A42B" zone (Virunga zone at a depth exceeding 30km).

The exploitation of the aforementioned hypothesis and our model made it possible to locate the main escaped faults and to note that:

- These faults are exactly located in areas with intense seismic activity; going deeper, these faults change position: the shape is no longer vertical or rectilinear, but wavy and serpentine.
- from the surface to a depth of 20 km, the faults of Kivu (A42) and Tanganyika (A43) zones are located near the rift, to move away from it beyond the depth of 20 km (corresponding to the position average of the Conrad discontinuity),
- While the position of the main faults at layer G (0-10 km) is located at A5 for seismic zone A42, these faults are located at zone A3 for A43 for the same layer (G) and the opposite at the layer C (10-20 km) and are all located at A1 beyond 20 km.

1. INTRODUCTION

The map in figure (2) from previous studies (Mukange, 2016; Mukange, 2021a,b) carried out on the characterization of the seismicity of the DRC and its surroundings reveals that:

- Seismic activity in the DRC is subdivided into two large zones:
- A non-rift zone (10°E-25°E) characterized by low seismicity,
- A rift zone (25°E-35°E) of high seismicity,
- A degree of heterogeneity of 65% and 55% following respectively the horizontal and vertical subdivision, i.e. an average degree of heterogeneity of 60%,
- Each grid zone (square with side 5°) has a degree of heterogeneity of 0%, i.e. homogeneous at 100%.
- Seismic activity is concentrated in the main faults,

The main objective of this work is to highlight the fine structure of the Rift zones. To do this, thanks to the design of the unified characterization scale based on the notion of seismic species, it will be necessary, on the one hand, to calculate the following parameters: the rate or degree of heterogeneity of the grid zones, their rate resemblance and conservation of seismic species and on the other hand, to precisely locate the main underground faults by positing the hypothesis that: "the main faults are located in places where the module of seismic activity is at paroxysm." The judicious exploitation of these parameters would allow better monitoring of geological phenomena and geodynamics, with an opening towards indirect geological prospecting.

The East African Rift System appears as a continental extension of the global system of lithospheric fractures which wind through the middle of the Atlantic and Indian Oceans and which extend into the eastern part of the African Continent via the Gulf of Aden and the Red Sea (Mukange, 2016; Boden et al. 1988; Bantidi, 2014a). This system of fractures is made up of two branches, namely:

- The eastern branch which, from the Afar triangle, crosses Ethiopia and Kenya to the northern Tanzanian divergence (Figure 1a); Mukange, 2012).

- The western branch is made up of a system of fractures which cross the garland of the Great Lakes, that is to say, from Lake Albert (617 m altitude) passes through Lakes Edouard (912m), Kivu (1462m), Tanganyika (780m), Rukwa (782m), Malawi (460m) and continues south to Mount Beira in Mozambique and southwest to Lake Kariba, Zimbabwe. This branch therefore covers most of the eastern provinces of the DRC from latitude 4°N to latitude 8°S. From the Red Sea to the Zambezi the East African Rifts cover more than 6000km long and 40 to 60km wide. The two branches split in two at the level of the Aswan lineament and join at the level of Lake Malawi (Figure 1a).

The seismic activity of the DRC also includes that characteristic of intra-plate fractures which thus affects the entire Congolese basin known as the “Congolese craton”.

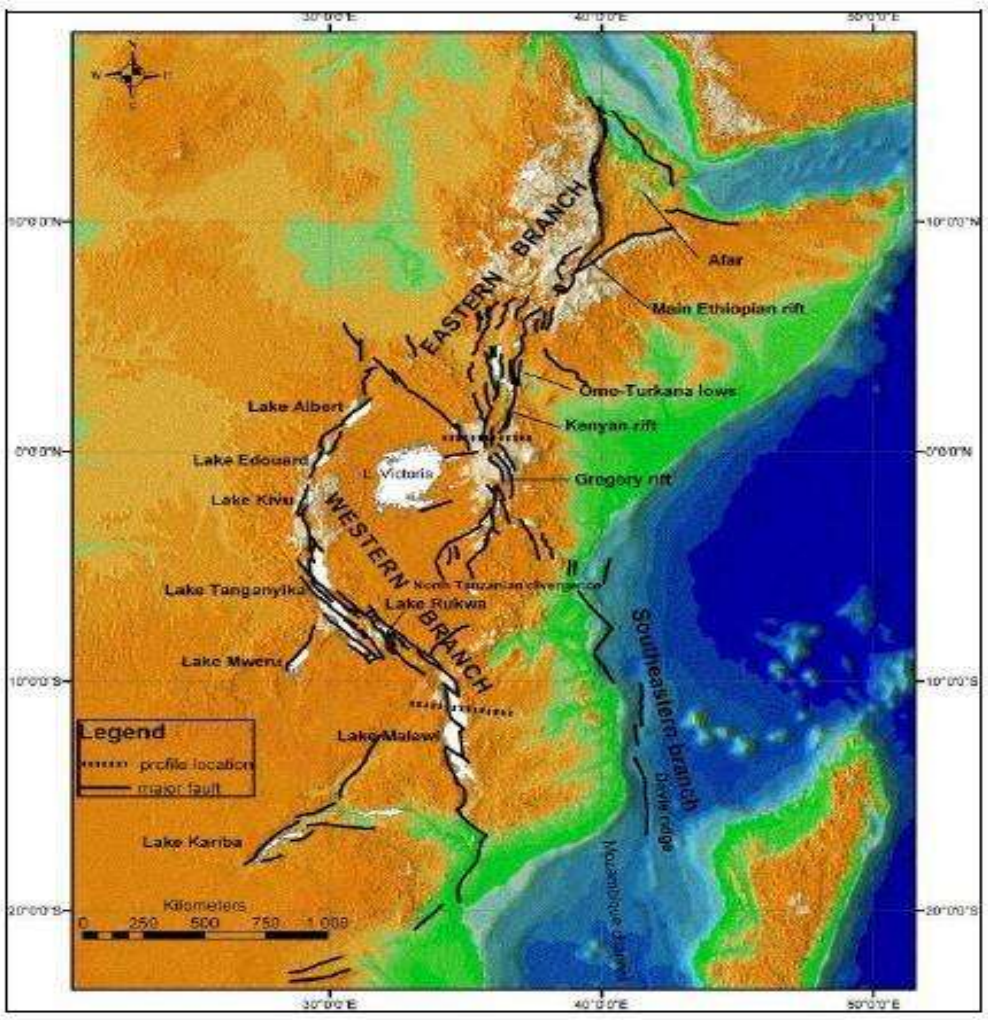

Figure 1a: The East African rift system (Mavonga, 2009)

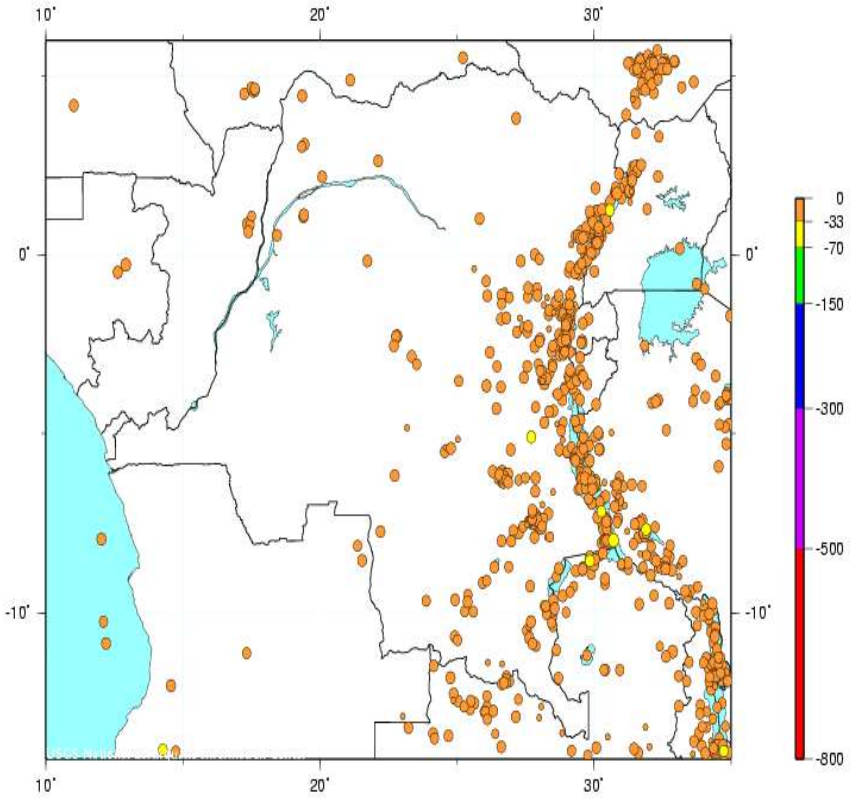

Fig. 1b: Distribution of epicenters in the DRC (1972-2008)

2. DATA AND METHOD OF ANALYSIS

This point is presented in two sub-points:

2.1. Analysis data

We analyze data collected through various sources (www.usgs.org and www.isc.ac.uk), covering the period from 1975 to 2013 over the geographical area between 6° North and 14° South latitude and between 25° East and 35° East longitude. This area includes the Rift grid zones A41, A42, A42, A44, A51, A52, A52 and A54 (figures 1b-2). Particular emphasis will be placed on zones A42, A42 and A44 located in the Congolese rift (Figure 1b).

2.2 Analysis method

Achieving our objectives requires the design of the unified characterization scale. This scale must integrate various classic parameters that we will have to calculate in each sub-zone; these are the following parameters:

- The total number of earthquakes,
- The total energy released by earthquakes,
- Maximum Magnitude,
- The maximum depth of the hypocenters,
- Surface area of each sub-zone,
- Volume of each subzone,
- Density of earthquakes,
- Energy density,
- The b-value (Lay and al., 1995) and the "d-value",
- The degree of heterogeneity of the area,
- The rate of resemblance of species,
- The conservation rate of species.

For explanations not provided here relating to the calculation of certain parameters, we invite the reader to consult the literature (Mukange, 2021a-b; Mukange 2023a-bc); this is particularly the case for the rate of heterogeneity.

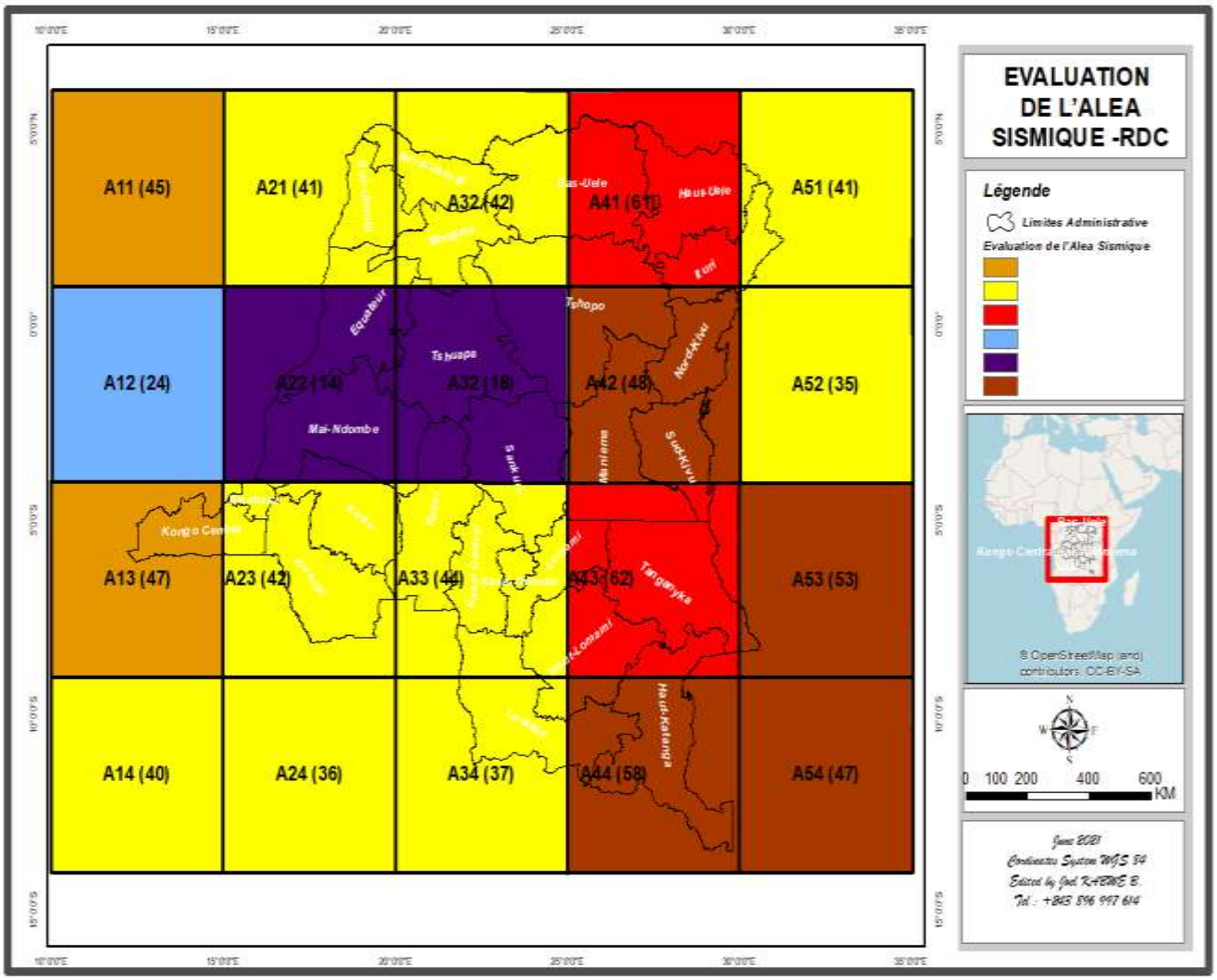

Figure 2: Seismic zoning in the Democratic Republic of Congo for seismic hazard assessment (Mukange, 2021b)

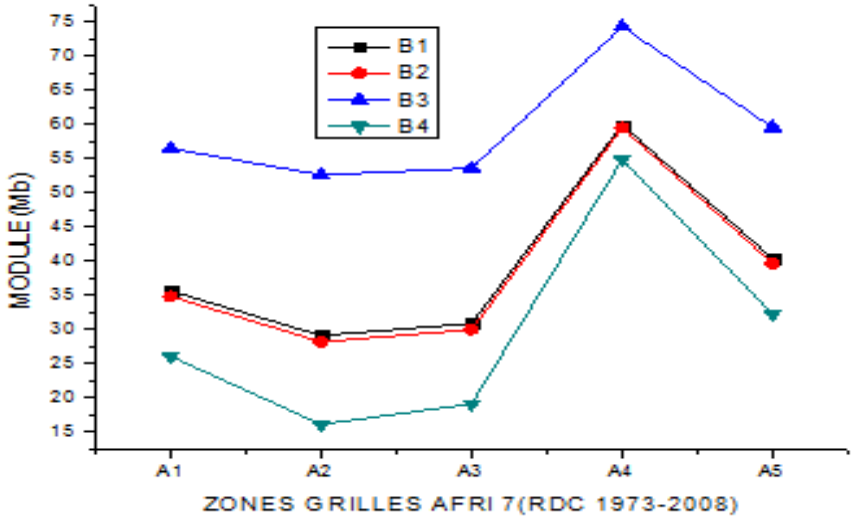

Figure 3 a: structural signature of the seismicity of the DRC

The map results above lead to obtaining the figure below called the structural signature of the seismic zone.

The characterization work will be carried out on each grid zone A41, A42, A43, A44, A51, A52, A52 and A54. Particular emphasis will be given to zones A42 and A43 due to the fact that one contains Lake Kivu in the Virunga volcano-seismic region, the other contains Lake Tanganyika in the Tanganyika seismic sub-zone (Mavonga, 2009; Figure 1).

The work of characterizing the internal structure of each of these zones therefore consists of:

- Subdivide each grid zone (Aij) according to depth (Table 3a); this slice is called depth zone,
- Subdivide each depth zone into vertical (Ai) and horizontal (Bj) sub-zones of one degree width (Table 2). Since each sub-zone Aij is a square of side 5°, by subdividing it thus, it will therefore be composed of twenty-five square sub-zones of side 1° each,
- Calculate the aforementioned characterization parameters in each Ai and Bj,
- Search for seismic species in each subzone Ai and Bj,
- Assign the seismic level and the appropriate color to each Ai and Bj,
- Calculate the module and assign the appropriate color to each grid zone Aij (Ai, Bj),
- Discuss and interpret the results,
- Draw the general conclusion and perspectives.

Table 1: **Boundaries of the DRC rift grid zones under study**

No.	AREA	LONGITUDE	LATITUDE
1	A42	25°E-30°E	1°N-4°S
2	A43	25°E-30°E	4°S-9°S
2	A44	25°E-30°E	9°S-14°S
4	A51	30°E-35°E	6°N-1°S
5	A52	30°E-35°E	1°N-4°S
6	A53	30°E-35°E	4°S-9°S
7	A54	30°E-35°E	9°S-14°S

Table 2: **Subdivision of zones (Aij) into vertical (Ai) and horizontal (Bj) sub-zones**

ZONE A42 (25°E-30°E; 1°N-4°S)			
No.	*ZONES Ai and Bj*	*LONGITUDE*	*LATITUDE*
01	A1	*25°E-26°E*	*1°N-4°S*
02	A2	*26°E-27°E*	*1°N-4°S*
02	A3	*27°E-28°E*	*1°N-4°S*
04	A4	*28°E-29°E*	*1°N-4°S*
05	A5	*29°E-20°E*	*1°N-4°S*
06	B1	*1°N-0°N(S)*	*25°E-20°E*
07	B2	*0°-1°S*	*25°E-20°E*
08	B3	*1°S-2°S*	*25°E-20°E*
09	B4	*2°S-2°S*	*25°E-20°E*
10	B5	*2°S-4°S*	*25°E-20°E*

Table 3: **Subdivision of zones (Aij) into depth zones for A42 and A43**

GRID AREA A42 AND A43			
No.	**ZONE-DEPTH**		**DEPTH SECTION (km)**
1	A42G	A43G	[0-10]
2	A42B	A43B	] 10-20]
2	A42B'	A43B'	] 20-20]
4	A42B''	A43B''	>20
5	A42C	A43C	] 0-20]
6	A42C'	A43C'	] 20-40]
7	A42C''	A43C''	>40

3. PRESENTATION AND DISCUSSION OF RESULTS

3.1. Presentation of the results

The values of the various calculated parameters are contained, for illustrative purposes for zone A42, in the table below

Table 4: Illustration of the parameters calculated in each sub-zone of zone Aij, case of A42

Below-Areas	b-value	λb-value	d-value	λd-value	Number (%)	Energy (%)	Magnitude maximum	Max hypocenter (km)	Volume density of earthquakes (%)	Energy volume density(%)
A1	0.669	1,541	0.0224	0.076	2.2	1.2	6.1	40	2.2	1.2
A2	1.0912	2,514	0.0126	0.021	8.2	0.1	5.4	96	17.0	0.2
At 3	0.9179	2,115	0.0492	0.112	9.4	20.8	5.5	25	52.6	119.0
A4	0.8262	1,904	0.046	0.105	11.2	12.0	6.4	40	56.2	65.1
AT 5	0.9706	2,226	0.0487	0.111	68.0	64.6	6.7	168	81.0	76.9
B1	0.999	2,202	0.045	0.102	27.9	10.4	6.2	168	45.2	12.4
B2	1.0526	2,425	0.046	0.105	14.6	0.2	5.5	85	24.2	0.6
B3	0.8865	2,042	0.0522	0.119	17.0	17.7	6.5	40	84.9	88.5
B4	0.9505	2,190	0.0477	0.108	14.8	9.4	6.4	46	64.2	40.8
B5	0.8227	1,919	0.024	0.055	15.8	41.7	6.7	96	22.8	86.8

3.2. Discussion of results

The discussion of the results is carried out in two main stages: the design of the unified characterization scale leading to the attribution of a seismic species to each sub-zone and the discussion itself (interpretation).

3.2.1. Design of the characterization scale

The characterization of the seismic activity of an area involves the design of a unified characterization scale which can reasonably integrate all the calculated parameters (Table 4). For this purpose, a characterization scale is developed consisting of five parameters and defined as follows:

X is the “form factor” which can take the value O, I, II, III, IV or V, with:

- 0 if the area is aseismic,

- I if the maximum magnitude recorded is between,
- II if the maximum magnitude recorded is between,
- III if the maximum recorded magnitude is between,
- IV if the maximum recorded magnitude is between,
- V if the maximum magnitude recorded is between,

The group of numbers (1; 2; 3; 4) in subscript constitutes the "structure factor", defined as follows:
the number 1 relates to the volume density of the seismic energy released in each sub-zone:

- if this density is ≤ 50%, then the number 1 takes the index "a",
- if this density is between 50% and 100%, then the number 1 takes the index "b",
- if this density is greater than 100%, then the number 1 takes the index "c",

the number 2 relates to the volume density of the number of earthquakes in each sub-zone:

- if this density is ≤ 50%, then the number 2 takes the index "a",
- if this density is between 50% and 100%, then the number 2 takes the index "b",
- if this density is > 100%, then the number 2 takes the index "c",

The number 3 relates to the λb-value parameter:

- If λb-value >2, then it takes the index "a",
- If 1< λb-value≤ 2, then it takes the index "b",
- If λb-value <1, then it takes the index "c",

Note that λb-value = 2.204 b-value. This parameter measures seismic activity.
The number 4 relates to the λd-value parameter:

- If the λd-value >0.2, then it takes the index "a",
- If the 0.1< λd-value≤ 0.2, then it takes the index "b",
- If the λd-value <0.1, then it takes the index "c",

Note that λd-value = 2.272d-value. This parameter is related to the structure of the soil.

3.2.2. Presentation of seismic species

The application of this scale to the various zones generates seismic species and levels (Tables 5-10). The seismic level is next to each seismic species. This scale also contains the seismic species discovered in the USA and Indonesia zone.

Table 5: Presentation of species and seismic level of each sub-zone

AREA DRC A42T	SEISMIC SPECIES		DRC ZONE A43T	SEISMIC SPECIES		DRC ZONE A44T	SEISMIC SPECIES		ZONE DRC A51T	SEISMIC SPECIES	
A1	IIIaabc	43	A1	IIabac	28	A1	IICCab	40	A1	IIIbbbC	61
A2	IIaaac	20	A2	IIaaaC	20	A2	IICabC	36	A2	IIIbCbC	65
A3	IIcbab	37	A3	IIIabbC	49	A3	IICbbC	38	A3	IVbCbC	82
A4	IIIbbbb	60	A4	IIabac	28	A4	IIabaC	28	A4	IaabC	4
A5	IIIbbab	59	A5	IIIccbb	75	A5	IIabaC	28	A5	IaabC	4
B1	IIIaaab	42	B1	IIaCab	22	B1	IICCaC	41	B1	IIIccbc	76
B2	IIaaab	18	B2	IIIccbb	75	B2	IIabbC	20	B2	IIIccbc	76
B3	IIIbbab	59	B2	IIIaCbb	52	B3	IICCab	40	B3	IVccab	82
B4	IIIabab	46	B4	IIIaCbb	52	B4	IICCaa	39	B4	IIabaC	28
B5	IIIbabc	56	B5	IIIaabC	44	B5	IIabaC	28	B5	IIabaC	28

Table 6: Presentation of species and seismic level of each sub-zone (continued)

ZONE DRC A42B	SEISMIC SPECIES		ZONE DRC A42B'	SEISMIC SPECIES		ZONE DRC A42B''	SEISMIC SPECIES		ZONE GROUND A43C''	SPECIES	
A1	IIaaaa	17	A1	IIaacb	25	A1	IIIcbbc	72	A1	0	0
A2	Iaaca	5	A2	IIaacb	25	A2	IIaabc	22	A2	0	0
A3	IIaaca	24	A3	IIaabb	22	A3	Iabbc	11	A3	0	0
A4	IIIbaba	55	A4	IIaaab	19	A4	IIacbc	25	A4	Iccbc	15
A5	IIIabba	47	A5	IIaabb	22	A5	IIIccac	75	A5	0	0
B1	IIIaaba	42	B1	IIaabb	22	B1	IIIccac	75	B1	0	0
B2	IIaaba	21	B2	IIaabb	22	B2	IIabbc	20	B2	Icccc	16
B3	IIIbaba	55	B3	IIaabb	22	B3	Iacac	12	B3	0	0
B4	IIaaba	21	B4	IIaabb	22	B4	IIIccbc	77	B4	Iaabc	4
B5	Yaaaa	1	B5	IIaaab	18	B5	IIaabc	22	B5	0	0

Table 7: Presentation of species and seismic level of each sub-zone (continued)

ZONE DRC A43B	SEISMIC SPECIES		ZONE DRC A43B'	SEISMIC SPECIES		ZONE DRC A43B''	SEISMIC SPECIES		ZONE DRC A42C	SEISMIC SPECIES	
A1	0aaaa	0	A1	0aaaa	0	A1	Iacba	14	A1	Iabaa	7
A2	Yaaaa	1	A2	Iaaba	3	A2	Iabba	9	A2	Yaaaa	1
A3	IIIbaca	58	A3	Iaaba	3	A3	Iabba	9	A3	Iabaa	7
A4	Iaaaa	1	A4	Iabba	9	A4	Iabbc	11	A4	IIIccaa	75
A5	IIIabba	48	A5	IIIbbca	65	A5	IIIacba	52	A5	IIIccaa	75
B1	IIaaba	21	B1	Iaaba	3	B1	IIabba	29	B1	IIIbcaa	66
B2	IIIaaca	46	B2	IIbbca	65	B2	IIacab	33	B2	IIabaa	26
B3	IIaaca	24	B3	IIaaca	24	B3	Iacab	13	B3	IIIcbaa	71
B4	IIaaca	24	B4	Iaaba	3	B4	IIIccca	80	B4	IIIbbaa	60
B5	IIIbaca	58	B5	Iaaba	3	B5	IIaaba	21	B5	IIIcbba	73

Table 8: Presentation of species and seismic level of each sub-zone (continued)

DRC ZONE A52T	SEISMIC SPECIES		ZONE DRC A53T	SEISMIC SPECIES		ZONE DRC A54T	SEISMIC SPECIES		ZONE DRC A42G	SEISMIC SPECIES	
A1	IIaCaC	22	A1	Ivbcbc	82	A1	IIabac	28	A1	IIaaac	20
A2	IIIcbbc	71	A2	IIIacbc	52	A2	IIIacbc	52	A2	IIaaac	20
A3	Iaaac	2	A3	Ivabbc	80	A3	IIabbc	20	A3	IIabac	28
A4	IIIccac	74	A4	IIaaac	20	A4	IIIacac	50	A4	IIIccbc	76
A5	IIaCaC	22	A5	IIIacbc	52	A5	IVccbc	84	A5	IIIbcac	64
B1	IIIcbbc	71	B1	IIacac	22	B1	IIIabbc	49	B1	IIIacac	50
B2	IIabac	28	B2	IVaabc	79	B2	IVccbc	84	B2	IIabac	28
B3	IIabac	28	B3	IIIacac	50	B3	IVccbc	84	B3	IIIcbac	69
B4	IIabac	28	B4	IVacbc	81	B4	IIacac	22	B4	IIIbbac	59
B5	IIIccac	74	B5	IIIabbc	49	B5	IIIacbc	52	B5	IIIcbbc	72

Table 9: Presentation of species and seismic level of each sub-zone (continued)

ZONE DRC A42C'	SEISMIC SPECIES		ZONE GROUND A42C''	SEISMIC SPECIES		ZONE DRC A43G	SEISMIC SPECIES		ZONE DRC A43C	SEISMIC SPECIES	
A1	IIIcabb	70	A1	Yaaaa	1	A1	IIaaac	20	A1	IIabac	28
A2	IIaabc	23	A2	0aaaa	0	A2	IIaaac	20	A2	IIaaab	19
A3	IIaabb	22	A3	0aaaa	0	A3	IIIbabc	56	A3	IIIcbba	72
A4	IIacab	33	A4	Iabbc	11	A4	IIaaac	20	A4	IIacaa	22
A5	IIIccab	76	A5	IIccbc	43	A5	IIIaaac	43	A5	IIIccaa	75
B1	IIIccab	76	B1	IIccbc	43	B1	IIaaac	20	B1	IIabab	27
B2	IIabbb	30	B2	IIaabc	23	B2	IIaabc	23	B2	IIIcbaa	71
B3	IIabbb	30	B3	IaDabc	4	B3	IIIbaac	55	B3	IIIccaa	75
B4	IIIabbb	50	B4	Iacbc	15	B4	IIaaac	20	B4	IIabaa	26
B5	IIabab	27	B5	Iaabc	4	B5	IIaaac	20	B5	IIIcbaa	71

Table 10: Presentation of seismic species and level of each sub-zone (end)

ZONE A43C'	A1		A2		A3		A4		A5	
SEISMIC SPECIES	Iabbc	11	Iabbc	11	Iabbc	11	Iabab	8	IIIccbb	78
ZONE A43C'	B1		B2		B3		B4		B5	
SEISMIC SPECIES	IIacbb	35	IIIcccb	81	IIabbc	31	IIIabbb	50	IIabbb	30

3.2.3. Calculation of the similarity rate

The rate of resemblance between two zones is done by comparing the respective seismic species or by setting a species taken as a unit of measurement (reference). The calculation is carried out as follows:

The characterization scale, giving rise to a seismic species, is written X1224. Let zones A and B have respective seismic species XA1A2A2A4A and XB1B2B2B4B. The resemblance rate is calculated based on the form factor (X) and the structure factor (1, 2, 3. 4) using the following formula:

Form factor

If , $X_A - X_B = 0$, then the resemblance rate is 50%,
If , $X_A - X_B = 1$, then the resemblance rate is 40%,
If , $X_A - X_B = 2$ then the resemblance rate is 30%,
If , $X_A - X_B = 3$, then the resemblance rate is 20%,
If , $X_A - X_B = 4$, then the resemblance rate is 10%,
If , $X_A - X_B = 5$, then the resemblance rate is 0%,

Structure factor

If , $1_A = 1_B$, then the resemblance rate is 15%, otherwise 0%
If , $2_A = 2_B$, then the resemblance rate is 15%, otherwise 0%
If , $3_A = 3_B$, then the resemblance rate is 10%, otherwise 0%
If , $4_A = 4_B$, then the resemblance rate is 10%, otherwise 0%

We see that the total is 100%.

Example: calculate the rate of resemblance between the zones characterized by the following species IVccba and Icbbc then calculate it by taking the species IVcccc as a unit of measurement (reference). The first rate is called the relative resemblance rate, the other is the absolute resemblance rate.

Example of calculating the relative similarity rate

Form factor

$IV_A - I_B = 2$, then the resemblance rate is 20%,
Structure factor

Like $1_A(c) = 1_B(c)$, then the resemblance rate is 15%,
Like $2_A(c) \neq 2_B(b)$, then the resemblance rate is 0%,
Like $3_A(b) = 3_B(b)$, then the resemblance rate is 10%,
Like $4_A(a) \neq 4_B(c)$, then the resemblance rate is 0%,

The total similarity rate is 45% (20%+15%+0%+10%+0%)

Example of calculating the absolute resemblance rate (we leave the task to the reader)

3.2.4. Results interpretation

The interpretation of the results focuses on the parameters below.

3.2.4.1. Seismic species, seismic levels and color

Observation of the results of tables (5-10) shows that:

- In total, we identified 89 distinct seismic species,
- There are 28 (42%) seismic species common to all areas,
- There are 17% of species exclusive to zones A51, A52, A52 and A54, zones between 30 and 35°E,
- There are 17% of seismic species exclusive to zone A42, subdivided into depth zones (A42G, A42B, A42B', A42B'', A42C, A42C', A42C'') according to table (3),
- There are 17% of species exclusive to zone A43, also subdivided into depth zones (A43G, A43B, A43B', A43B'', A43C, A43C', A43C'').

The statistics indicate:

- The first zone (A4j) is less seismic than the second (A5j): one having a form factor (III), the other (IV); As a result, we see that their intersection is empty (figure 3b),

- The resemblance rate, based on structural factors, between these two zones is 17%: there is one common element out of a total of six (Figure 3c),

- The structure of the DRC (25°-30°E) is more stable than that of Malawi-Zambezi (30°E-35°E),

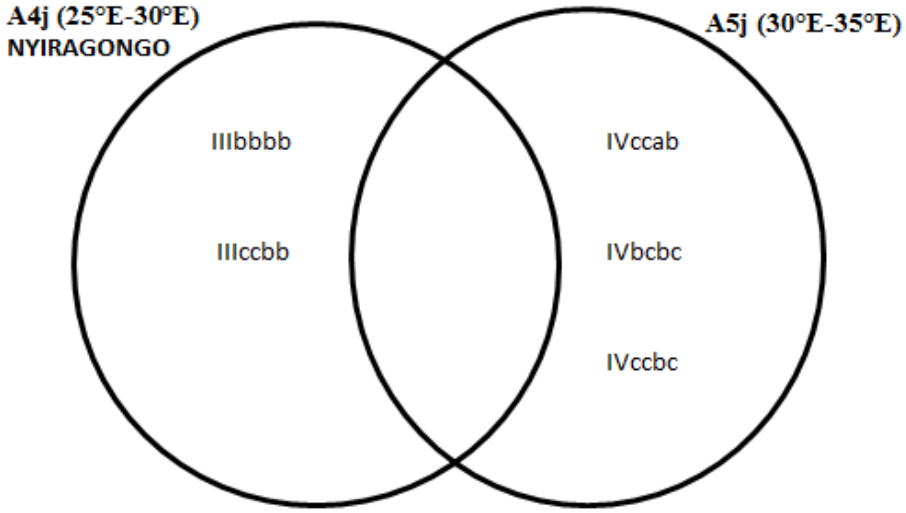

Figure 3b: comparison of seismic species between the two zones of the A4j rift (25°E-30°E) and A5d (30°E-35°E)

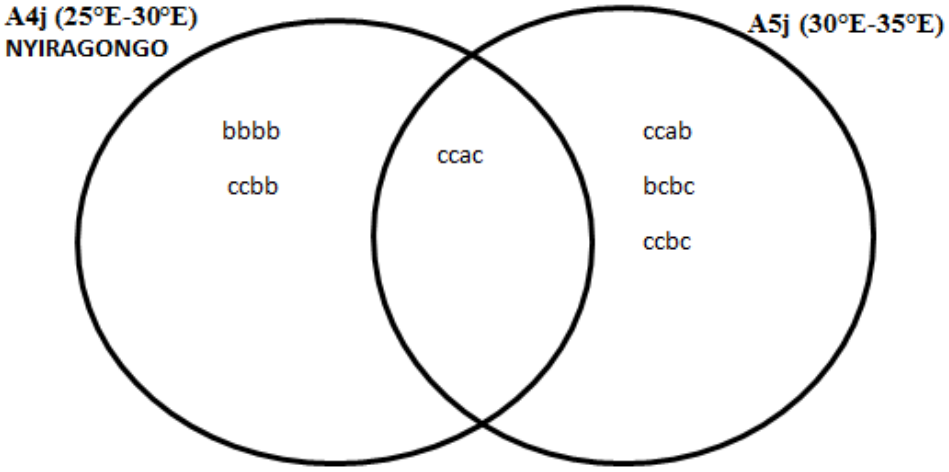

Figure 3c: comparison of the structure factors between the two zones of the A4j rift (25°E-30°E) and A5d (30°E-35°E)

3.2.4.2. Seismic zoning of grid zones

The notion of grid zones (Aij) is related to that of vector representation (Mukange, 2021a-b)

The module (c) of each subzone Cij is calculated using the formula (2.12)
Or, and correspond respectively to the seismic levels of the vertical subzones (Ai) and (Bj) contained in tables (5-10).

Table 11: Color code relating to module slice and quantum level

MODULE (c)	QUANTUM LEVEL	COLORS
0	0	BLACK
]0,15]	1	PURPLE
]15,30]	2	LIGHT BLUE
]30,45]	3	DARK BLUE
]45,60]	4	LIGHT GREEN
]60,75]	5	DARK GREEN
]75,90]	6	YELLOW
]90,105]	7	ORANGE
]105,120]	8	LIGHT RED
]120,135]	9	DARK RED

The application of this code to each zone, and for illustration purposes to zone A42, leads to the results contained in the Table below.

Table 12: Illustration of the results from the previous table for the A42T zone

Area DRC A42T	Seismic level of Ai	Seismic level of Bi	Module of Aij (Ai,Bj)	Quantum level	Color code	Color statistics
A11	42	42	60	4	LIGHT GREEN	28%
A12	42	18	47	4	LIGHT GREEN	28%
A13	42	59	72	5	DARK GREEN	44%
A14	42	46	62	5	DARK GREEN	44%
A15	42	56	71	5	DARK GREEN	44%
A21	20	42	47	4	LIGHT GREEN	4%
A22	20	18	27	2	LIGHT BLUE	4%
A23	20	59	62	5	DARK GREEN	44%
A24	20	46	50	4	LIGHT GREEN	4%
A25	20	56	59	4	LIGHT GREEN	4%
A31	27	42	56	4	LIGHT GREEN	4%
A32	27	18	41	3	PURPLE	4%
A33	27	59	70	5	DARK GREEN	44%
A34	27	46	59	4	LIGHT GREEN	4%
A35	27	56	67	5	DARK GREEN	44%
A41	60	42	72	5	DARK GREEN	44%
A42	60	18	62	5	DARK GREEN	44%
A43	60	59	84	6	YELLOW	20%
A44	60	46	76	6	YELLOW	20%
A45	60	56	82	6	YELLOW	20%
A51	59	42	72	5	DARK GREEN	44%
A52	59	18	62	5	DARK GREEN	44%
A53	59	59	82	6	YELLOW	20%
A54	59	46	75	5	DARK GREEN	44%
A55	59	56	81	6	YELLOW	20%

The results in the table above and others in the appendix lead to the highlighting of zoning maps, representing the chromatic structure of seismic zones.
NB: Each sub-zone delimited by color is a square with a side of one degree (1°).

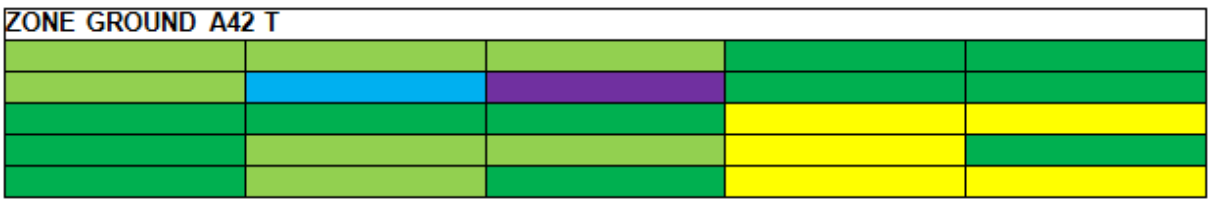

Figure 4a: Seismic zoning map of the DRC A42T zone

Figure 4b: Seismic zoning map of the DRC A43T zone

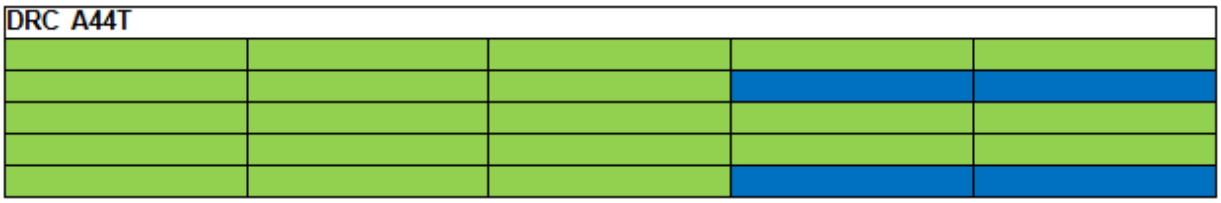

Figure 4c: Seismic zoning map of the DRC A44T zone

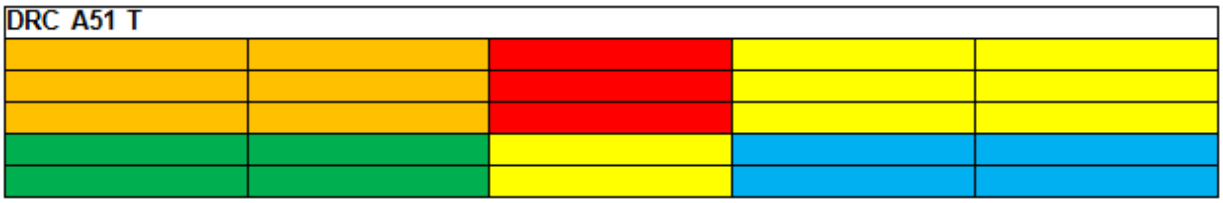

Figure 4d: Seismic zoning map of the DRC A51T zone

Figure 4e: Seismic zoning map of the DRC A52T zone

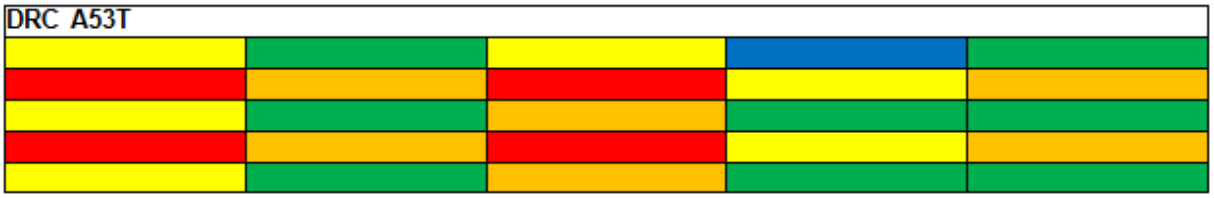

Figure 4f: Seismic zoning map of the DRC A53T zone

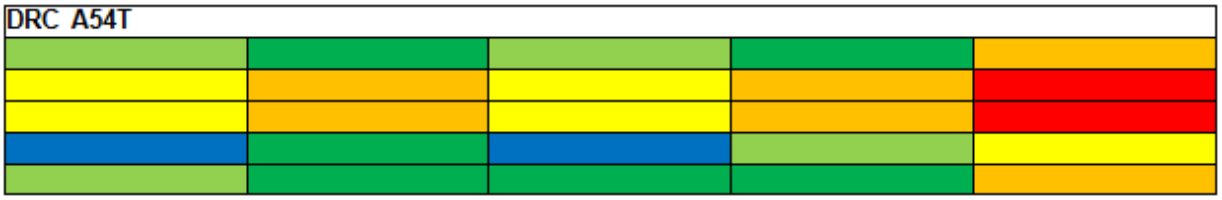

Figure 4g: Seismic zoning map of the DRC A54T zone

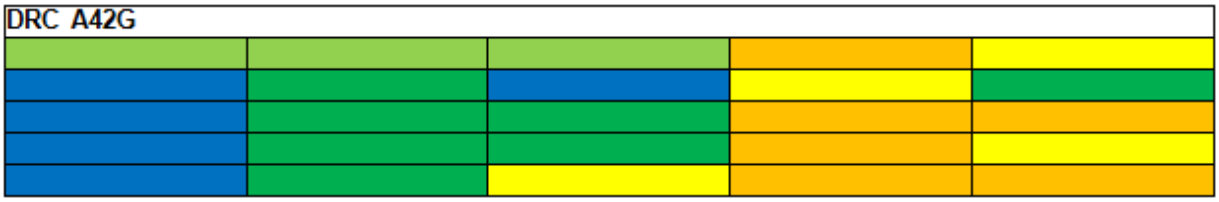

Figure 4h: Seismic zoning map of the DRC A42G zone

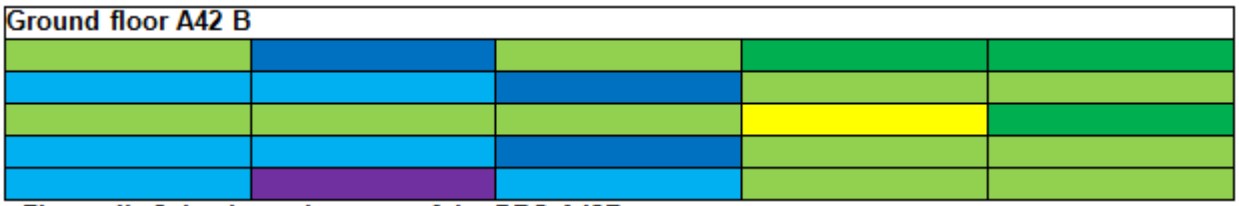

Figure 4i: Seismic zoning map of the DRC A42B zone

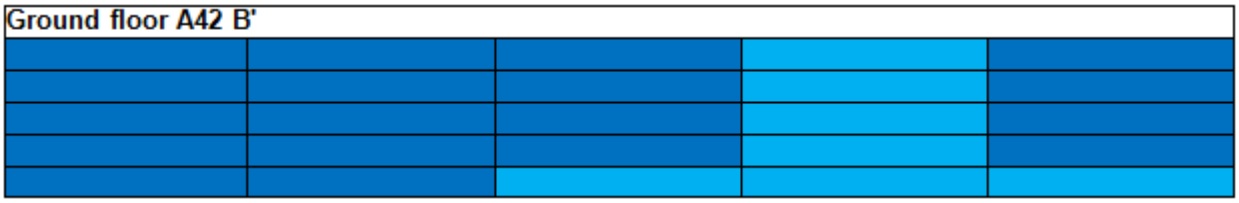

Figure 4j: Seismic zoning map of the DRC A42B' zone

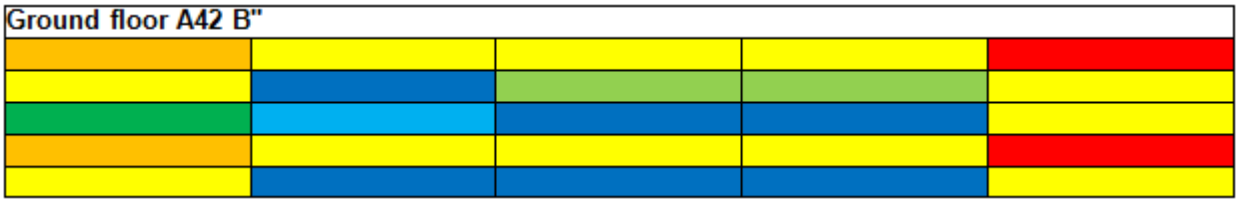

Figure 4k: Seismic zoning map of the DRC A42B'' zone

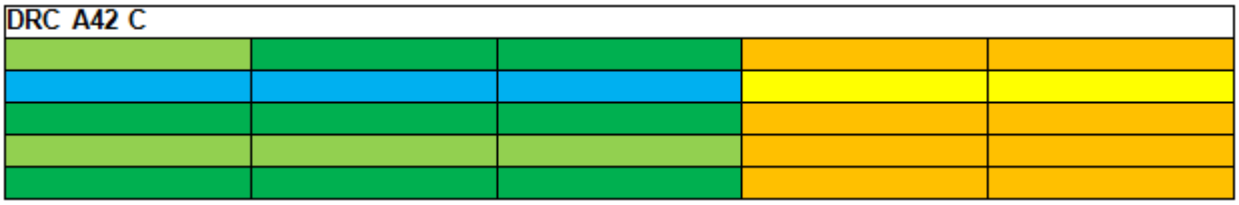

Figure 4l: Seismic zoning map of the DRC A42C zone

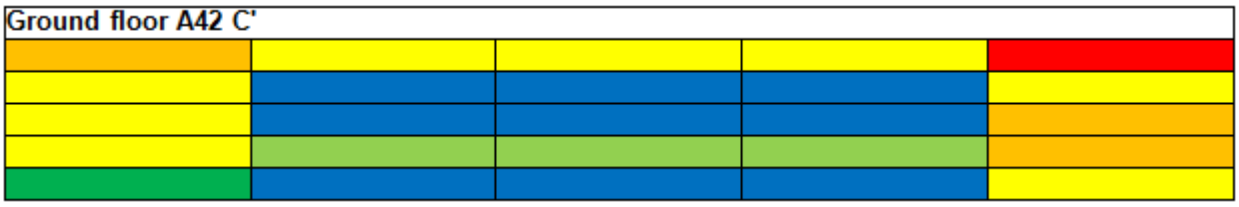

Figure 4m: Seismic zoning map of the DRC A42C' zone

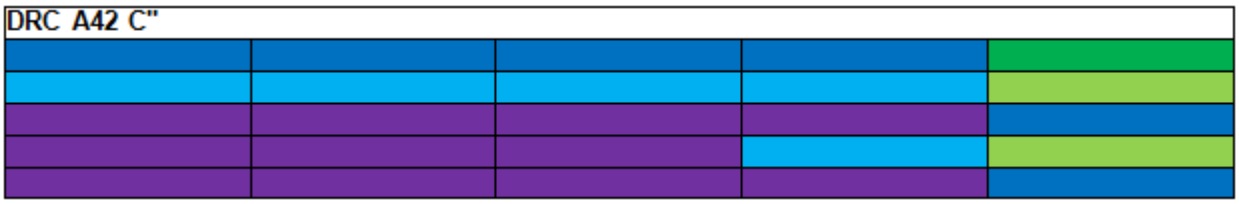

Figure 4n: Seismic zoning map of the DRC A42C zone

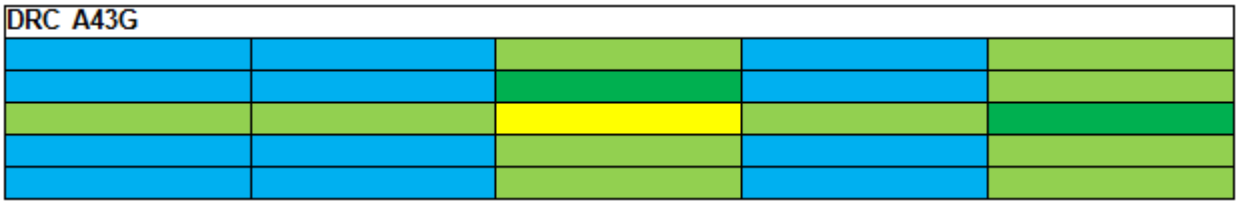

Figure 4o: Seismic zoning map of the DRC A43 G zone

Figure 4p: Seismic zoning map of the DRC A43B zone

Figure 4q: Seismic zoning map of the DRC A43B' zone

Figure 4r: Seismic zoning map of the DRC A43B'' zone

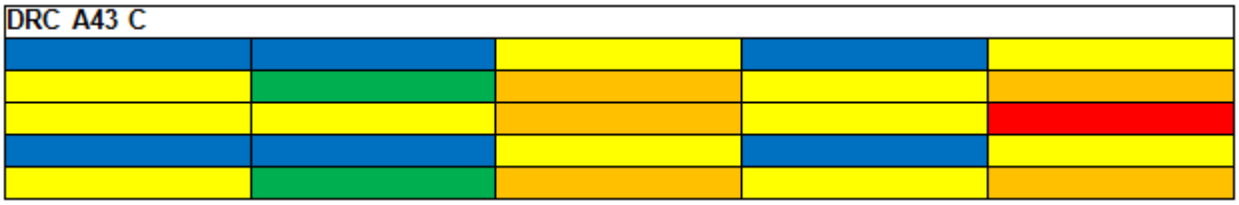

Figure 4s: Seismic zoning map of the DRC A43C zone

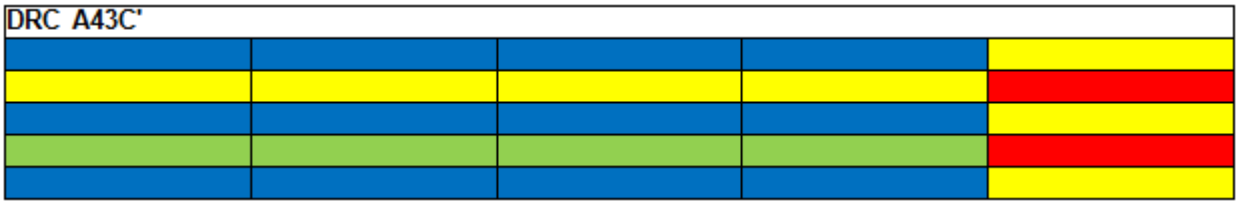

Figure 4t: Seismic zoning map of the DRC A43C' zone

Figure 4u: Seismic zoning map of the DRC A43C' zone

Depending on the color arrangements, we observe that all these 21 zones are grouped into two shapes:

- A symmetrical shape of the colors in relation to zone A3; these are zones A51T, A52T, A53T and A54T located between 30° and 35°E,
- A bipolar form (two groups of colors) for all areas located between 25° and 20°E; these are the A42T, A43T, A44T and their derivatives.

3.2.4.3. Calculation of the degree of heterogeneity and the rate of resemblance

The degree or rate of heterogeneity is calculated by taking the ratio, as a percentage, of the total number of colors identified in the area to ten colors retained in the color code (Figures 4). The resemblance rate is calculated according to the formula indicated in point (2.2.2). However, we distinguish two similarity rates (TR):

- The first, called absolute (TR1): this is the resemblance between the maximum seismic species taken as a reference and the maximum species observed among the Ai and Bj of the zone where we want to evaluate the rate (Tables 5-10 ; Tables 13-14),
- The second, called relative (TR2) or cumulative calculated according to the depth of the layers going from the surface downwards (Tables 15-16).

Table 13: Calculation of the absolute resemblance rate for A42 zones

No.	AREAS TO COMPARE	RESEMBLANCE RATE (TR1)
0	A42T-A42T	100%
1	A42T-A42G	60%
2	A42T-A42B	75%
3	A42T-A42B'	50%
4	A42T-A42B"	60%
5	A42T-A42C	50%
6	A42T-A42 C'	60%
7	A42T-A42 C"	50%

Table 14: Calculation of the absolute resemblance rate for A43 zones

No.	AREAS TO COMPARE	RESEMBLANCE RATE (TR1)
0	A43T-A43T	100%
1	A43T-A43G	60%
2	A43T-A43B	50%
3	A43T-A43B'	50%
4	A43T-A43B"	80%
5	A43T-A43C	80%
6	A43T-A43 C'	90%
7	A43T-A43 C"	60%

Table 15: Calculation of the relative similarity rate for A42 zones

No.	AREAS TO COMPARE	RESEMBLANCE RATE (TR2)
0	A42T-A42T	100%
1	A42T-A42G	60%
2	A42G-A42B	60%
3	A42B-A42B'	55%
4	A42B'-A42B"	40%
5	A42B"-A42C	80%
6	A42C-A42 C'	90%
7	A42C'-A42 C"	80%

Table 16: Calculation of the relative similarity rate for A43 zones

No.	AREAS TO COMPARE	RESEMBLANCE RATE (TR2)
0	A43T-A43T	100%
1	A43T-A43G	60%
2	A43G-A43B	65%
3	A43B-A43B'	85%
4	A43B'-A43B"	60%
5	A43B"-A43C	90%
6	A43C-A43C'	80%
7	A43C'-A43 C"	70%

The figure below shows the distribution of similarity and heterogeneity rates for each zone.

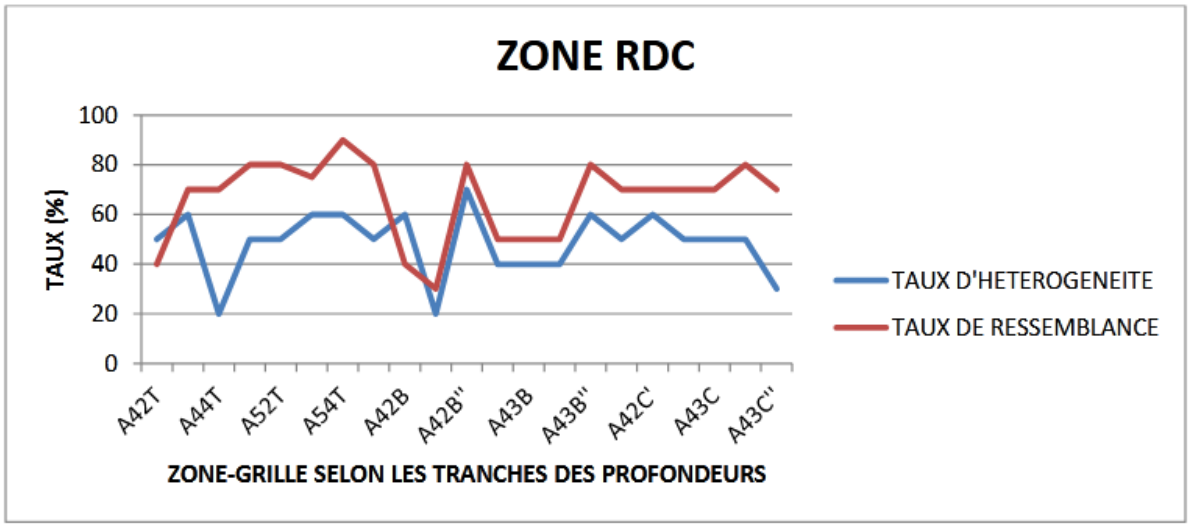

Figure 5: Distribution of the absolute heterogeneity and resemblance rate according to the zones

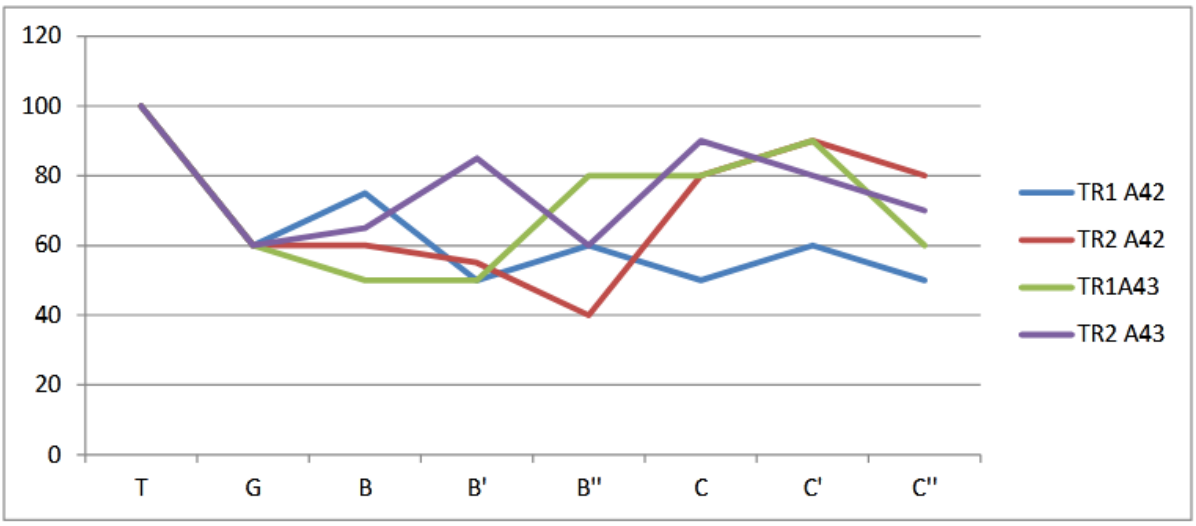

Figure 6a: Distribution of absolute (TR1) and relative (TR2) resemblance rates according to zones A42 and A43

From these curves, the following observations emerge:

- With a few exceptions, there is a correlation between the absolute resemblance rate (TR1) and the relative resemblance rate (TR2), (Figure 6);
- With a few exceptions, except at A42G and A42B, there is a correlation between the absolute or relative rate of resemblance and the rate of heterogeneity (Figure 5);
- There is a correlation between the number of curves and the rate of heterogeneity; in fact, we see that the number of curves decreases with the rate of heterogeneity: at less than 50% of this rate, there are at most three structural curves (Figure 5 and Figures 7).
- As a result, another heterogeneity rate can be calculated based on the number of visible curves (out of five in total) on the structural curves (geo-seismic signature, figures 7a-l)

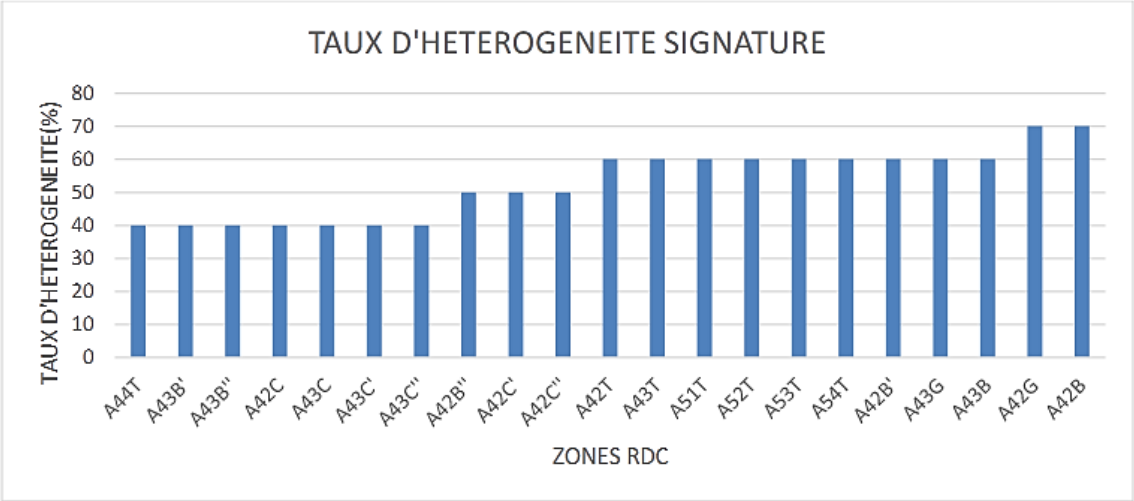

Figure 6b: Heterogeneity rate calculated based on geo-seismic signatures

The figure above groups the zones into four classes, made up of zones with a rate of 40%, 50%; 60% and 70% whose distribution of zones is represented by the graph below.

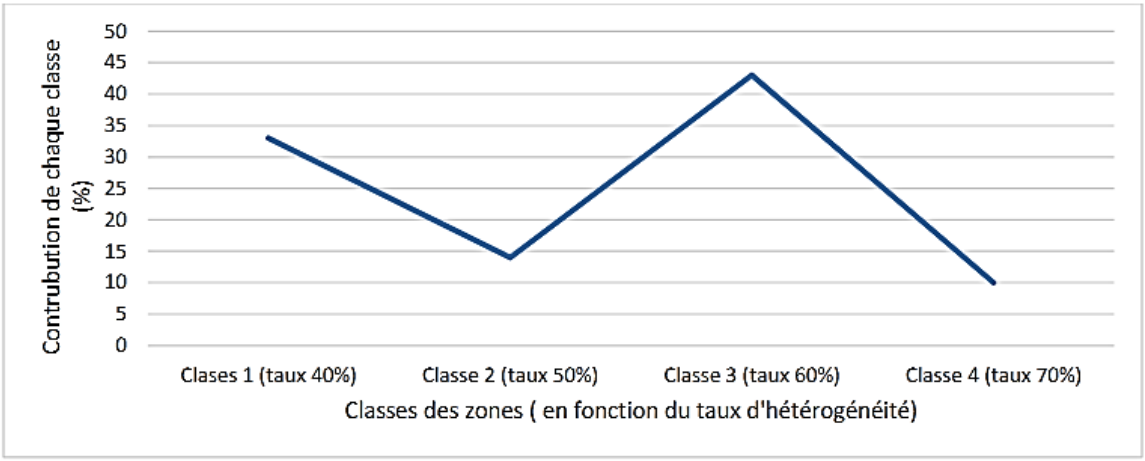

Figure 6c: Weight of each class made up of zones according to the level of heterogeneity rate of geoseismic signatures

We see that classes (1 and 3, odd) are dominant; they cover 76% of the areas

3.2.4.3. Species conservation rate

Calculating the conservation rate of species (Tables 17-20), inverse of the disappearance rate, consists of comparing the common species between two zones. Each zone has, at most, ten seismic species (Tables 5-10)

Table 17: Calculation of the absolute conservation rate of the species for A42 zones

No.	AREAS TO COMPARE	CONSERVED SPECIES	CONSERVATION RATE	DISAPPEARANCE RATE
1	A42T-A42G	Ilaaac	10%	90%
2	A42T-A42B	None	0%	100%
3	A42T-A42B'	Ilaaab	10%	90%
4	A42T-A42B''	None	0%	100%

Table 18: Calculation of the absolute conservation rate of the species for A43 zones

No.	AREAS TO COMPARE	CONSERVED SPECIES	CONSERVATION RATE	DISAPPEARANCE RATE
1	A43T-A43G	Ilaaac	10%	90%
2	A43T-A43B	None	0%	100%
3	A43T-A43B'	None	0%	100%
4	A43T-A43B''	Ilacab	10%	90%

The tables above calculate the conservation rate of the zones step by step (relative rate)

Table 19: Calculation of the relative conservation rate of the species for A42 zones

No.	AREAS TO COMPARE	CONSERVED SPECIES	CONSERVATION RATE	DISAPPEARANCE RATE
1	A42T-A42G	Ilaaac	10%	90%
2	A42G-A42B	None	0%	100%
3	A42B-A42B'	None	0%	100%
4	A42B'-A42B''	None	0%	100%

Table 20: Calculation of the relative conservation rate of the species for A43 zones

No.	AREAS TO COMPARE	CONSERVED SPECIES	CONSERVATION RATE	DISAPPEARANCE RATE
1	A43T-A43G	Ilaaac	10%	90%
2	A43G-A43B	None	0%	100%
3	A43B-A43B'	0aaaa, Ilaaca	20%	80%
4	A43B'-A43B''	labba	0%	100%

These tables indicate an average conservation rate of 5%, 5%, 2.5% and 5% for figures (17-20) respectively. We conclude that species are rarely preserved as a function of depth.

3.2.4.4. Structural curve (geo-seismic signature)

The results in table (12) and others in the appendix, in particular, have been transformed into the curves below, called “geo-seismic signatures” or “structural signatures”. The geodynamics of an area can be monitored based on the variation of the signature over time.

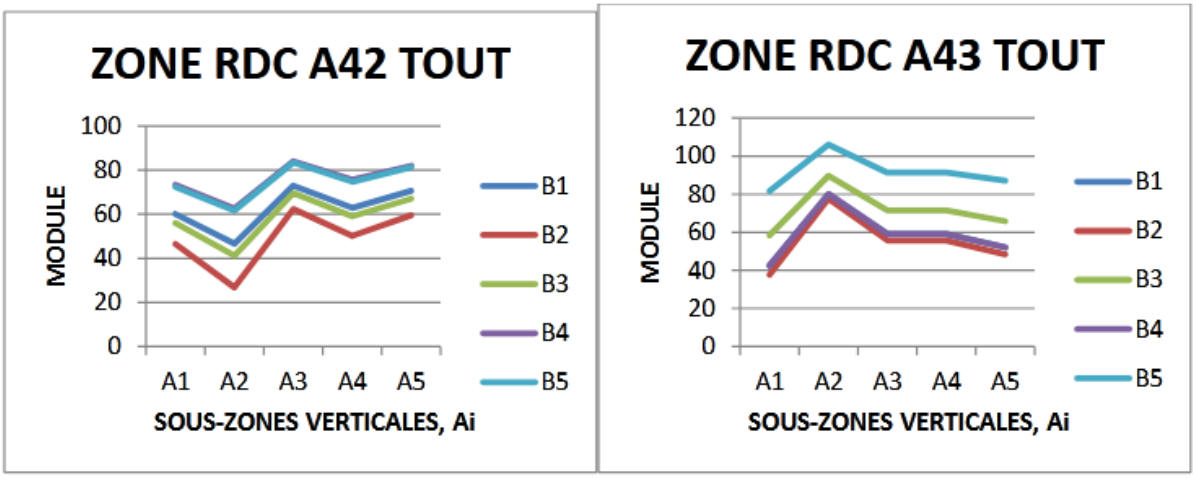

Figure 7a: Structural curves (signature) of zones A42T and A43T

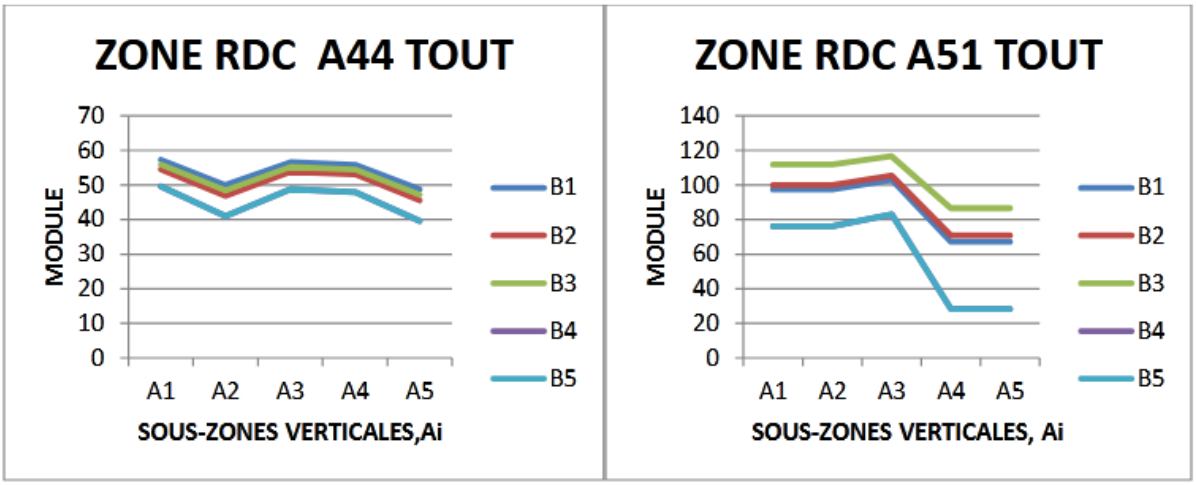

Figure 7b: Structural curves (signature) of zones A44T and A51T

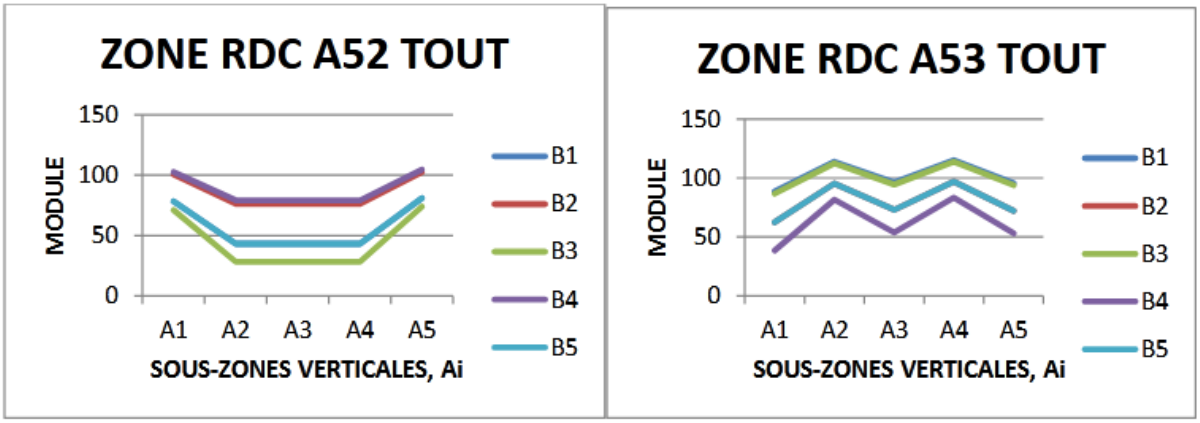

Figure 7c: Structural curves (signature) of zones A52T and A53T

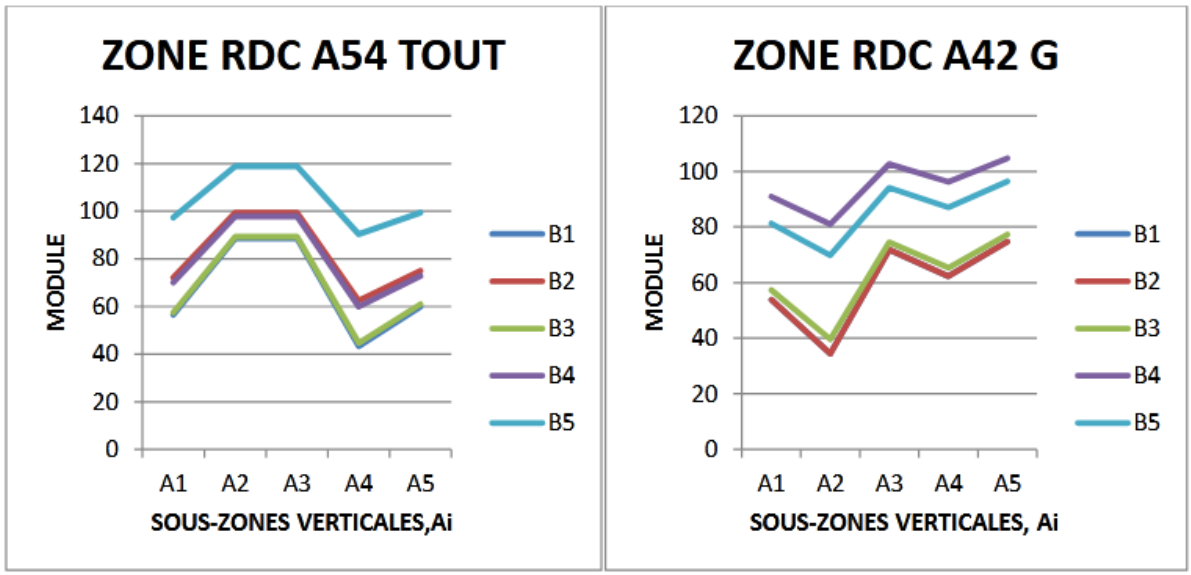

Figure 7d: Structural curves (signature) of zones A54T and A42G

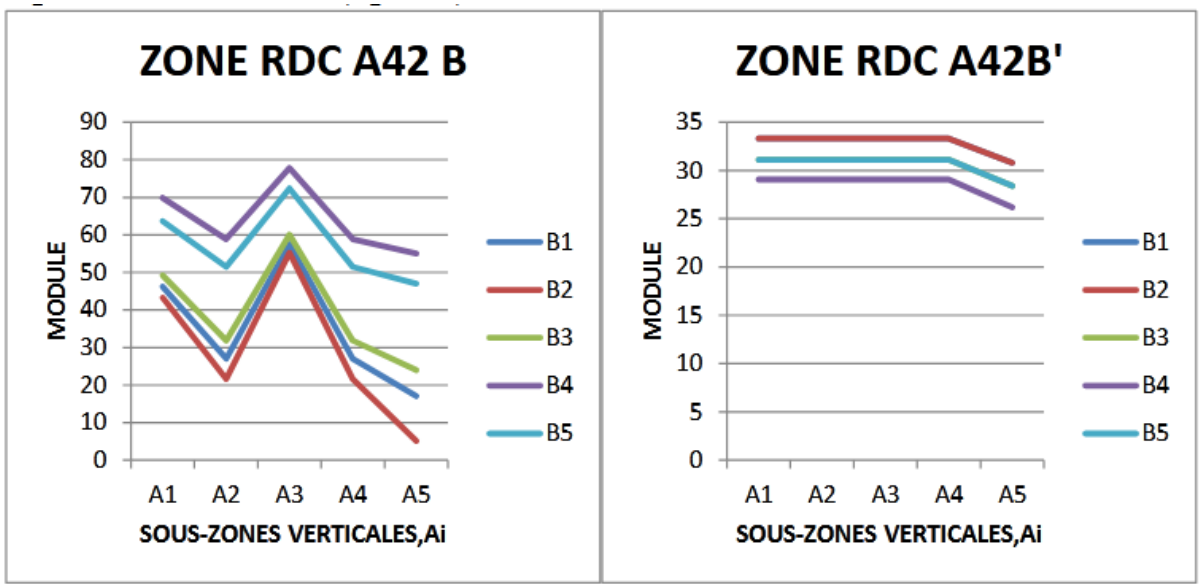

Figure 7e: Structural curves (signature) of zones A42B and A42B'

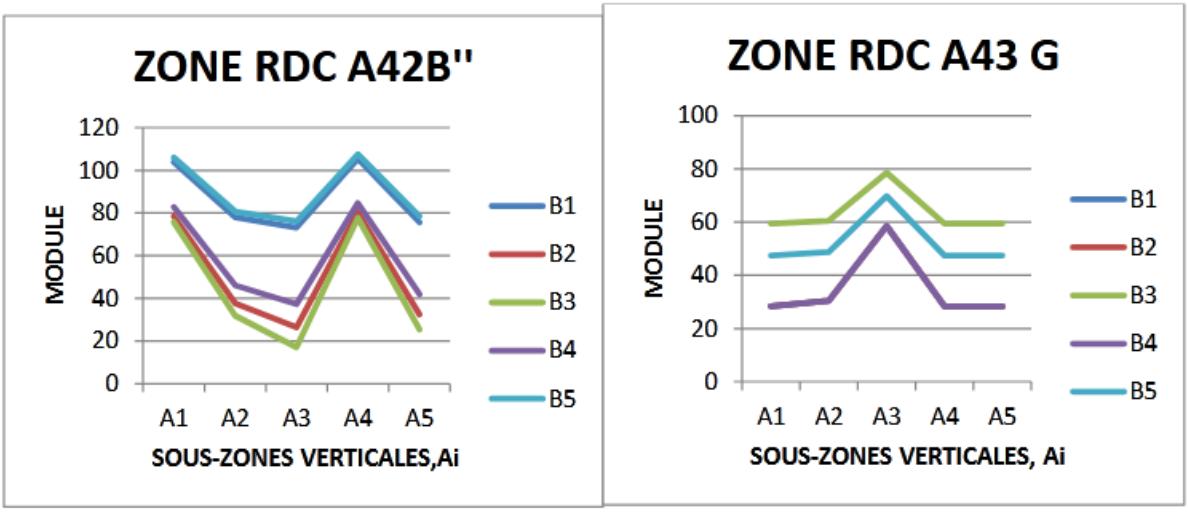

Figure 7f: Structural curves (signature) of zones A42B'' and A43G

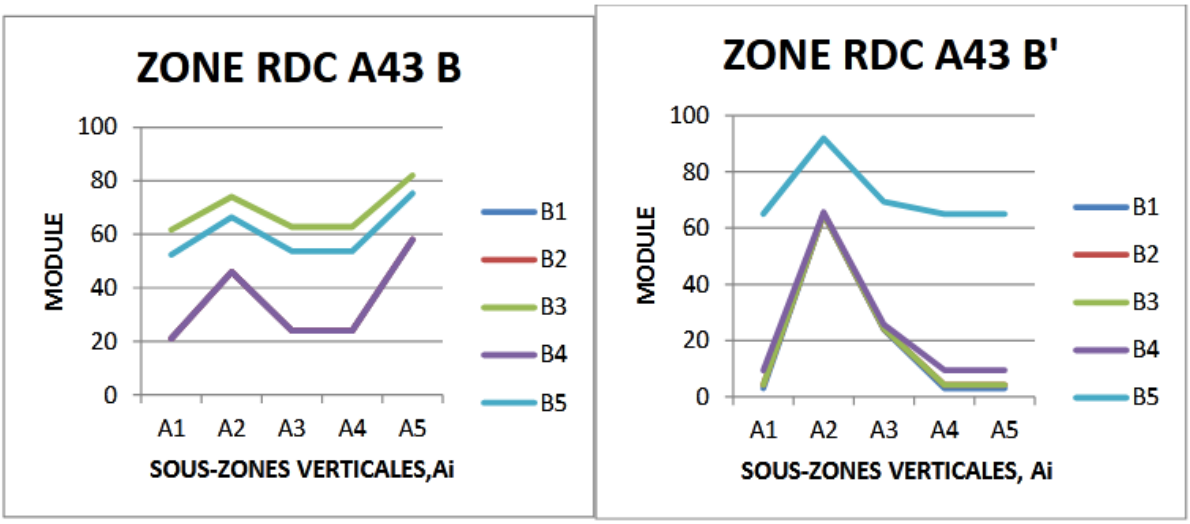

Figure 7g: Structural curves (signature) of zones A43B and A43B'

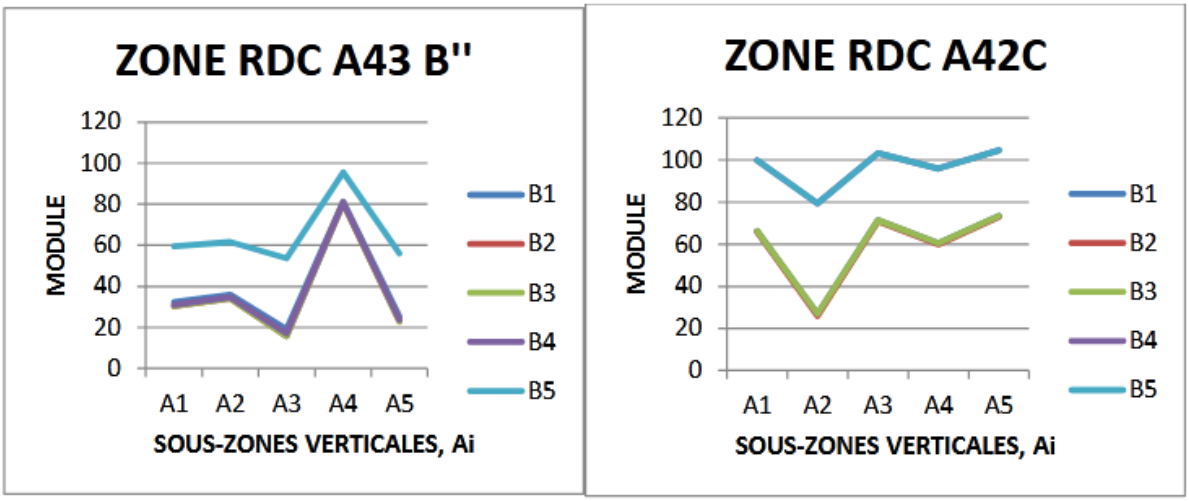

Figure 7h: Structural curves (signature) of zones A43B'' and A42

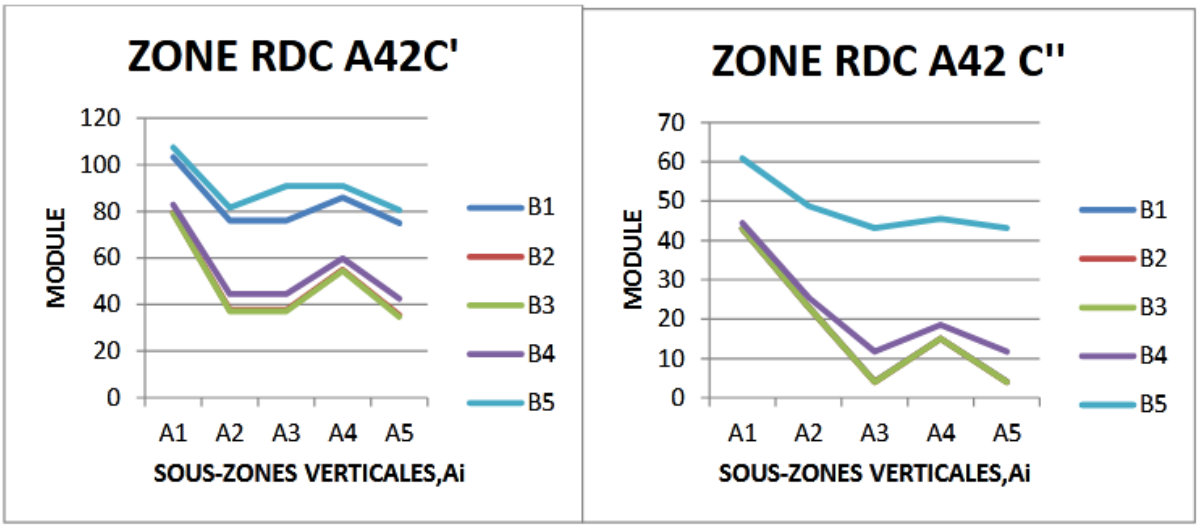

Figure 7i: Structural curves (signature) of zones A42C' and A42C''

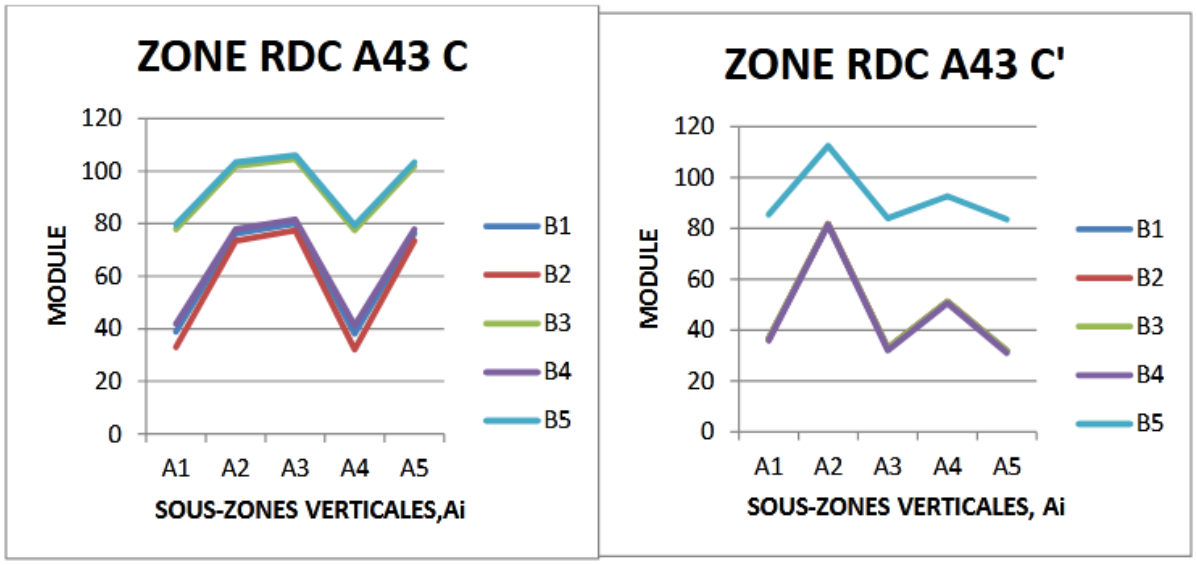

Figure 7j: Structural curves (signature) of zones A43C and A43C'

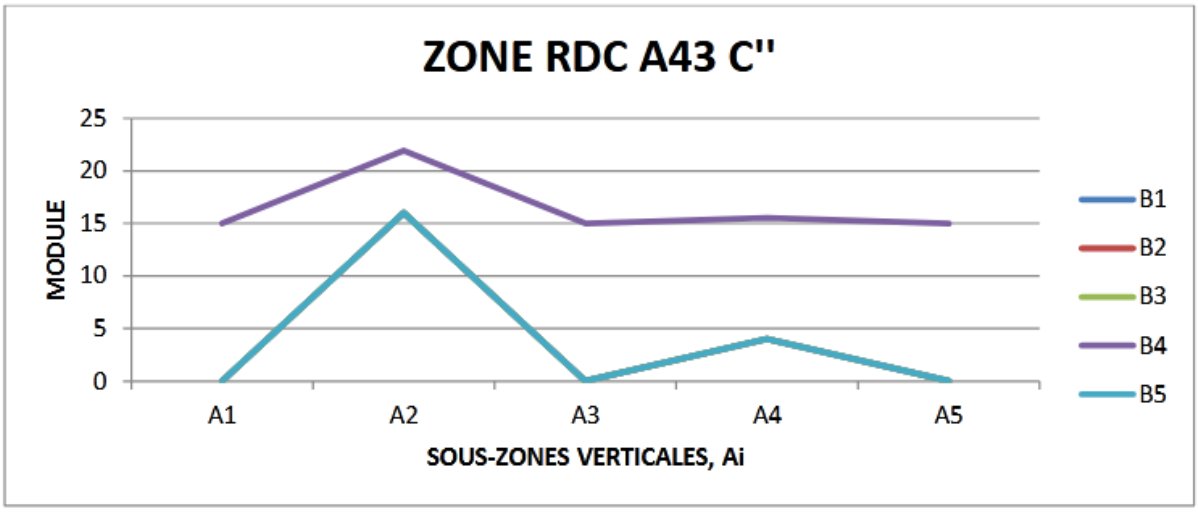

Figure 7k: Structure curves (signature) of A43C'' zones

The observation of these signatures groups them into five modes (Table 21).

Table 21: classification of zones according to the modes or shapes of the structural curves

Fashion	Straight upward sloping (positive)	Straight downhill (negative)	Concavity curve turned downwards	Concavity curve turned upwards	Mixed concavity
Areas	A42G, A42C	A44T, A51T, A42B', A42C,' A42C''	A42T, A43T, A54T, A42B, A43G, A42C, A42G, A43B', A43B''	A52T	A53T,A42G,A42B'',A43B,A42C
Statistics	9.1%	22.7%	40.9%	4.6%	22.7%

Statistics indicate that:

- The majority (41%) of structures are in the category of downward-facing concavity curves,
- Zones A42 (G and C) and A52T are singularities; remember that zone A42 is located in the Virunga-Lake Kivu volcanic region and that zone A52 is to its right (Figure 2).

3.2.4.5. Comparison of some structures

Among the structures above, there are those that attract our attention; in fact we see that:

- The two structures below have the same shape or mode with concavity facing upwards, but symmetrical: the final part of the curves of one is worth the initial part for the other and vice versa; simply turn one over and superimpose it on the other to have identical structures.

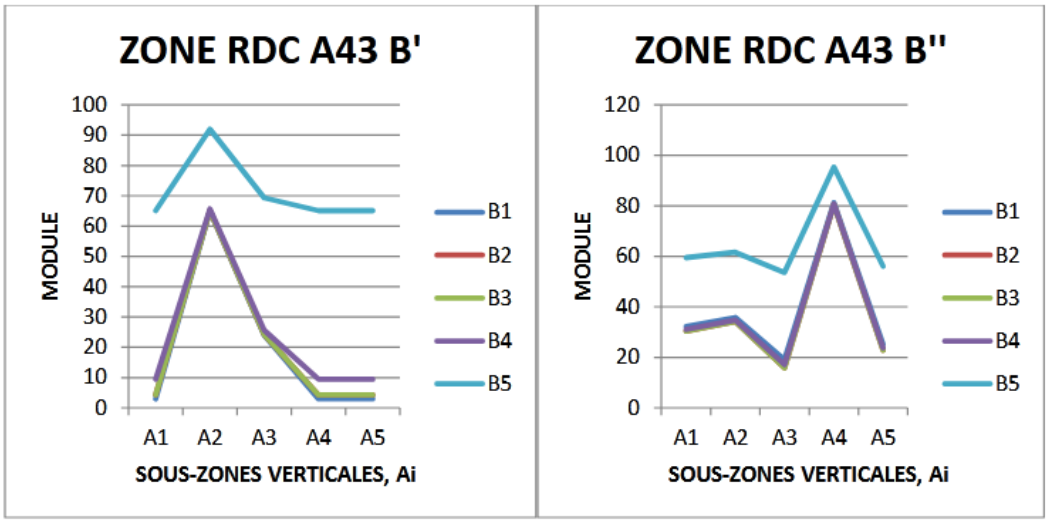

Figure 8a: comparison of the structural curves of zones A43B' and A43B''

What has just been observed above is also valid for the two structures below.
NB: A42 (Virunga-Kivu) and A43 (Tanganyika).

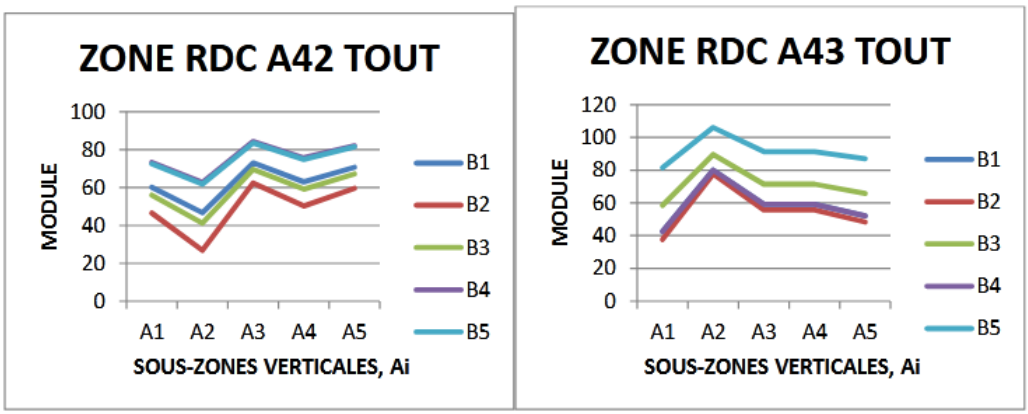

Figure 8b: comparison of the structure curves of zones A42T and A43T

We observe that the structure of zone A44 (Upemba rift zone, Haut-Katanga region) straddles A42T and A43T. These nuances are also observed in relation to the orientations of the main faults (Figure 9).

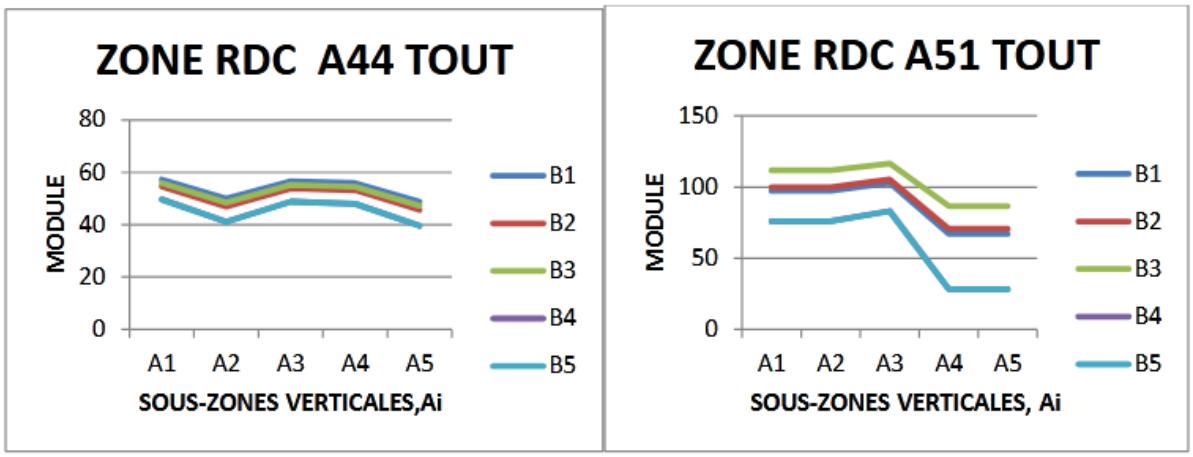

Figure 8c: comparison of the structural curves of zones A44T and A51T

Overall its two structures below are the opposite of one (concavity upwards) of the other (concavity downwards);

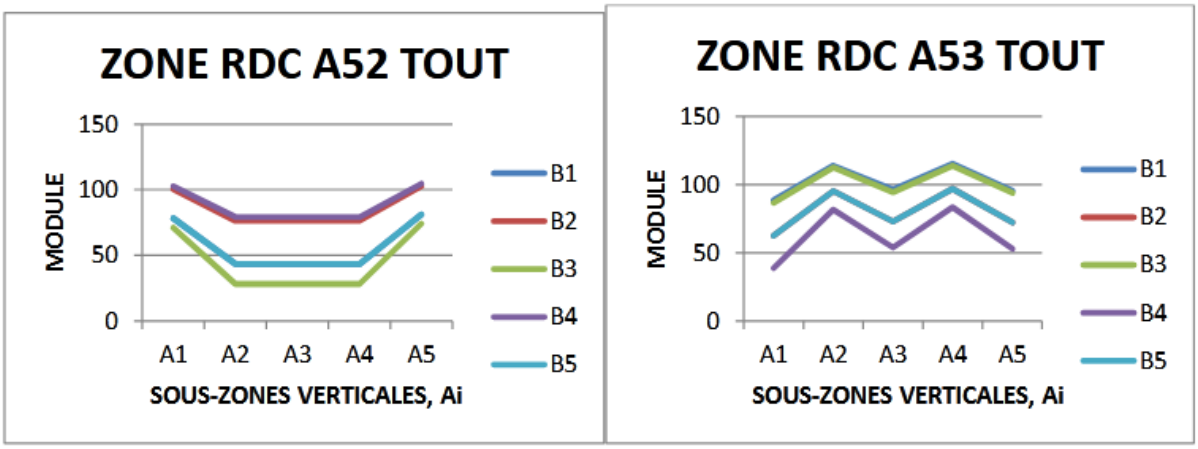

Figure 8d: comparison of the structure curves of zones A52T and A53T

The following two structures are so similar that we can affirm that the entire structure of the DRC (10-35°E, 6°N-14°S) is dictated by that of the A42B'' zone (Virunga zone at depth exceeding 30km);

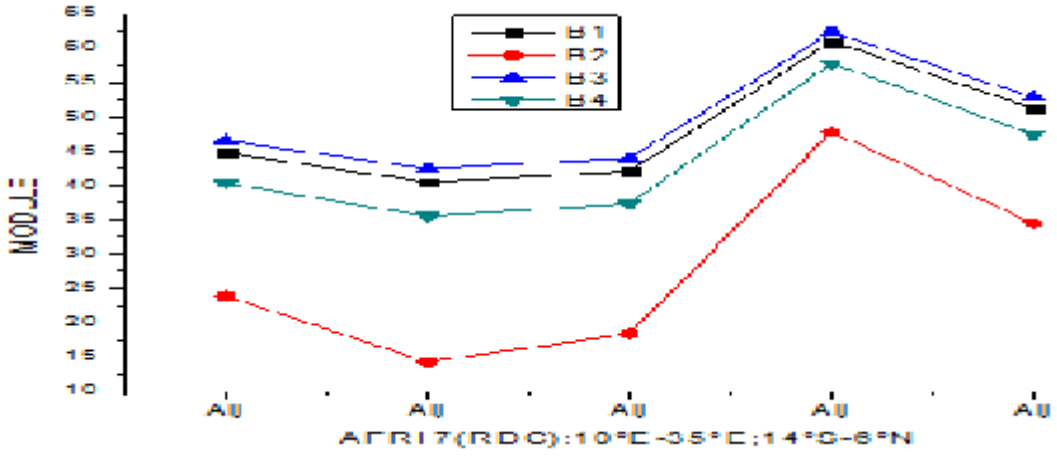

Figure 8e: comparison of the structure curves of the A4B'' zones and the DRC (all)

These two structures below are similar, yet we observed that their total structures (A42T and A43T, figure 8b) are opposite or symmetrical; this shows that the orientations of the main faults of these two zones are sometimes parallel, sometimes crossed at certain depths (Figure 9).

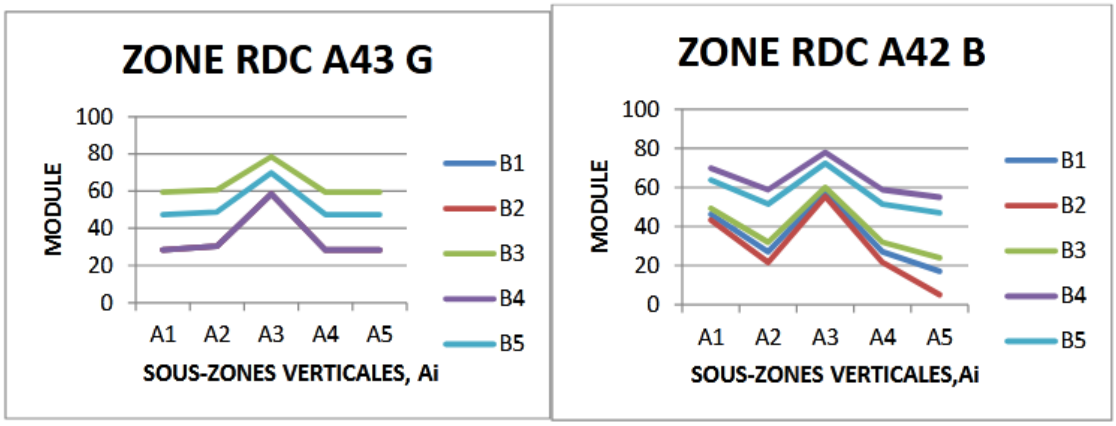

Figure 8f: comparison of the structural curves of zones A43G and A42B

Indeed, the geological overview of the DRC shows that this territory has the following characteristics (Figure 1 and 9):

- In the eastern part of the western branch of the East African Rift system, a network of main faults winds from north to south, from Lake Albert in the north to Lake Tanganyika in the south. From the southern end of Lake Tanganyika, the fault system extends in a southwest direction towards Lake Moero and Lake Upemba, then, in a southeast direction towards Lake Rukwa and Malawi (Figure 2.3),
- Other faults have been highlighted in the north-western part of the DRC, in the territory of Ubangi, in the province of Equateur, and extends into the Central African Republic, towards Bangui its capital,
- In the Kongo central province(Bas Congo), in the west of the DRC, the structural map of the DRC highlights the presence of faults; it is the same in the North-East of the DRC, in Orientale Province.
- However, Lake Kivu is at the crossroads of two directions (South-West and South-East).

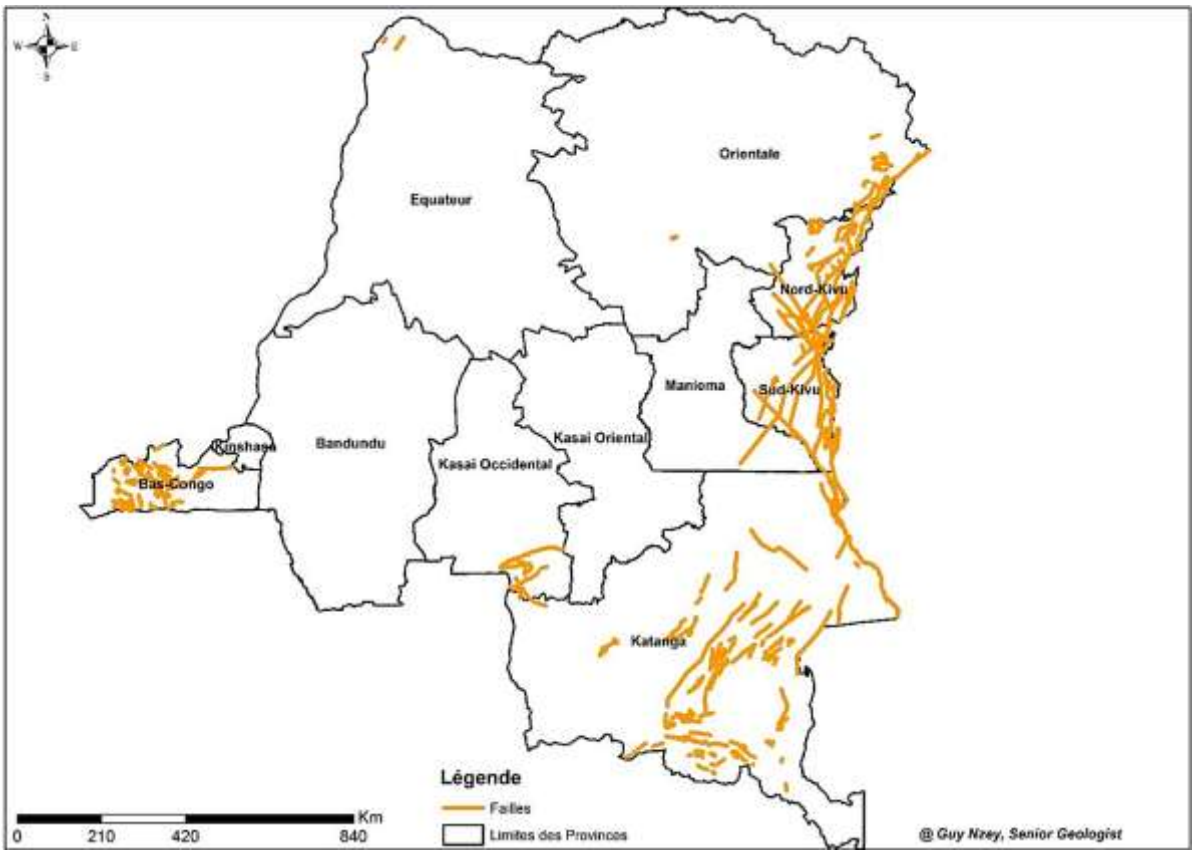

Figure 9: Structural map of the DRC (CRGM): the yellow lines represent the main faults

3.2.4.6. Comparison of zones based on horizontal and vertical subzones

The comparison uses the following histograms

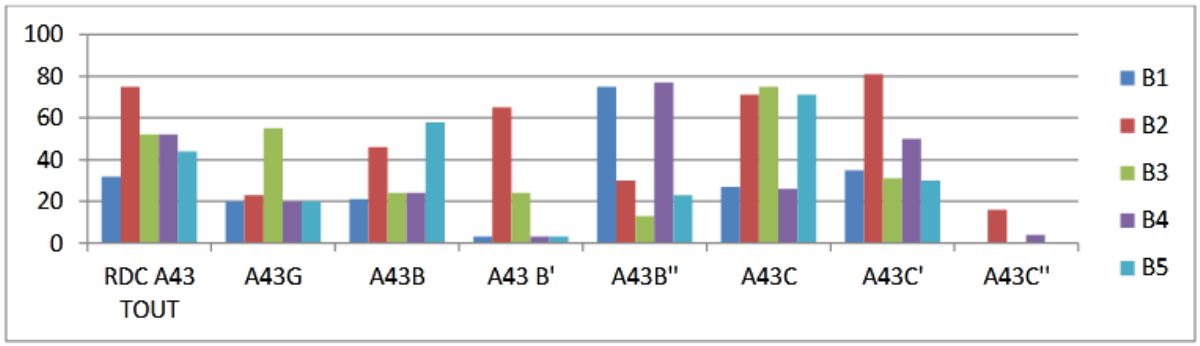

Figure 10a: Distribution of seismic levels of horizontal zones (Bj) by seismic zone A43

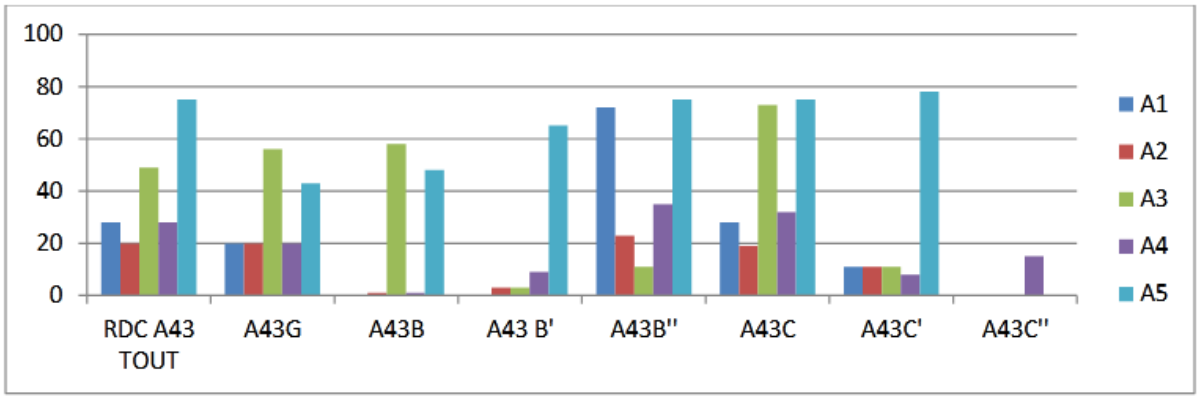

Figure 10b: Distribution of seismic levels of vertical zones (Ai) by seismic zone A43

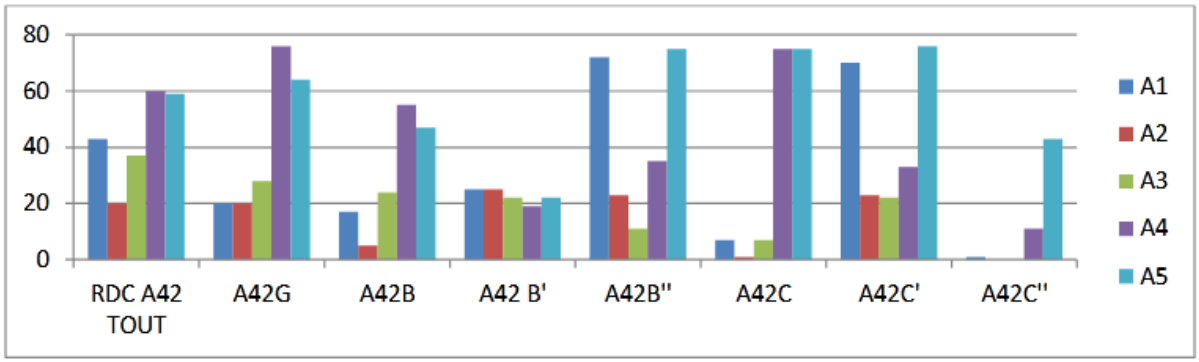

Figure 11a: Distribution of seismic levels of vertical zones (Ai) by seismic zone A42

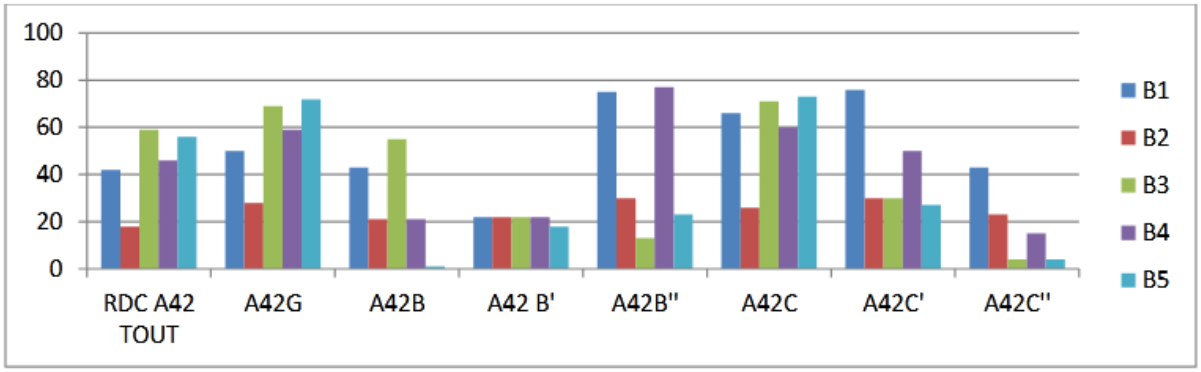

Figure 11b: Distribution of seismic levels of horizontal zones (Bj) by seismic zone A42

From these figures, we draw the following conclusions:

- A43T is similar to A43C based on vertical subzones (Ai),
- A43T is similar to A43C' based on the horizontal sub-zones (Bi),
- A42T is similar to A42B based on vertical subzones (Ai),
- A42T is similar to A42C based on horizontal subzones (Bi),

The data in Table (12) and others in the appendix can be grouped into classes; These include statistics on the weight of each color (module) in the zoning maps (Figures 4). Table (21) therefore groups the zones according to classes (in steps of fifteen); we obtain six classes, one of which is empty

Indeed, we call the modulus gap the difference between the maximum and minimum modulus of the zone.

3.2.4.7. Final structures

Table 21: classification of zones according to the gap relative to the weight of the colors

No. (class)	Module Gap Interval	Affected areas	Number of zones (%)
1	0-15	A42B'	4.7
2	15-30	A43C'', A44T	9.4
3	30-45		0
4	45-60	A43G, A42T, A42''	14
5	60-75	A43B, A43T, A42G, A42C',A42B, A43C	29
6	75-90	A53T, A54T, A52T A43B'', A42C, A43C', A51T, A43B,'A42B''	43

The six classes can again be grouped into three:

- An exceptional group including the zones of classes 1 and 2 with 14% of the zones: this group only includes the derivatives of the zones of the Tanganyika region (A43 C''), Virunga-Lake Kivu (A42B') and the rift of Upemba-Haut Katanga (A44T),
- An intermediate group, 43%, made up of classes 4 and 5: there we find the zones derived from A42 and A43, as well as A42T and A43T,
- A final group made up of class 6 which weighs 43%: this group includes all four zones between 30 and 35°E (A51T, A52T, A53T and A54T) and some derivatives of A42 and A43

Overall, these criteria highlight a clear distinction between the zones of the Congolese rift (A42, A43 and A44: 25-30°E) and that of the Malawi-Zambezi rift (A51, A52, A53 A54: 30-35°E).

The combination of the similarity rate, heterogeneity and color gap parameters for each zone gives them the final structures presented below

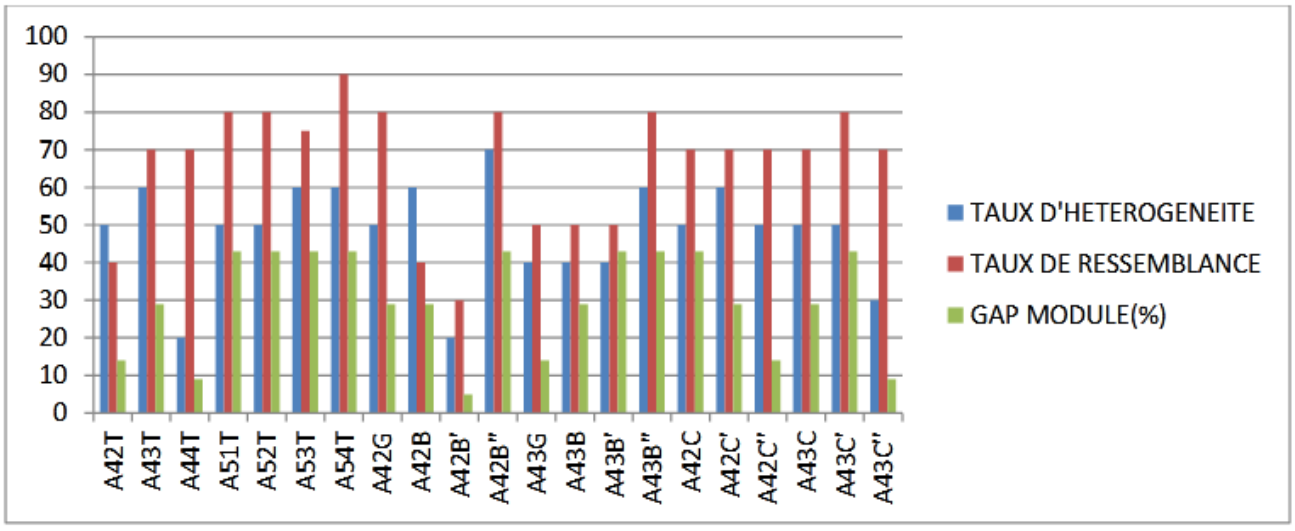

Figure 12a: Distribution of parameters in legend by seismic zone

Observation of these structures (figure 10) groups them into three classes;

Table 22: classification of zones according to figure (10)

No. (class)	Affected areas	Weight(%)
1	A43T, A44T A52T,A53T,A51T,A54T,A42B'',A42B',A42B'',A42G,A43G,A43B,A43B'', A42C,A42C',A42C'',A43C,A43C',A43C''	85
2	A42B, A42T	10
3	A43B'	05

The analysis also integrating the heterogeneity rate parameter based on the geo-seismic signature (figure 10b) highlights two groups:

- One, composed of areas located between 30 and 35°E (A51T, A52T, A53T and A54T),
- The other consists of zones between 25 and 30°E (A42, A43 and A44T), in the Congolese rift.

However, depending on one or another parameter, these zones have some nuances:

- ❖ The A44T zone (in the Upemba rift) tends to separate from A42T (Virunga zone) to get closer to A43T (Tanganyika zone),
- ❖ The A42T zone, if not alone, is sometimes close to the A5j zones. The A44T area seems to act as a hinge or suture zone between the two groups ( ). The structural map (Figure 9) is in agreement with the aforementioned observations, particularly with regard to the orientations of the main faults (Figure 9).

3.2.4.8. Comparison of zones based on b-value and d-value parameters

These parameters will allow us to model the structures in order to follow the geodynamic evolution. Remember that the b-value parameter measures the seismic activity of an area, while the d-value measures the internal structure (of the soil).

The search for the establishment of a correlation between these two parameters provided the following curves.

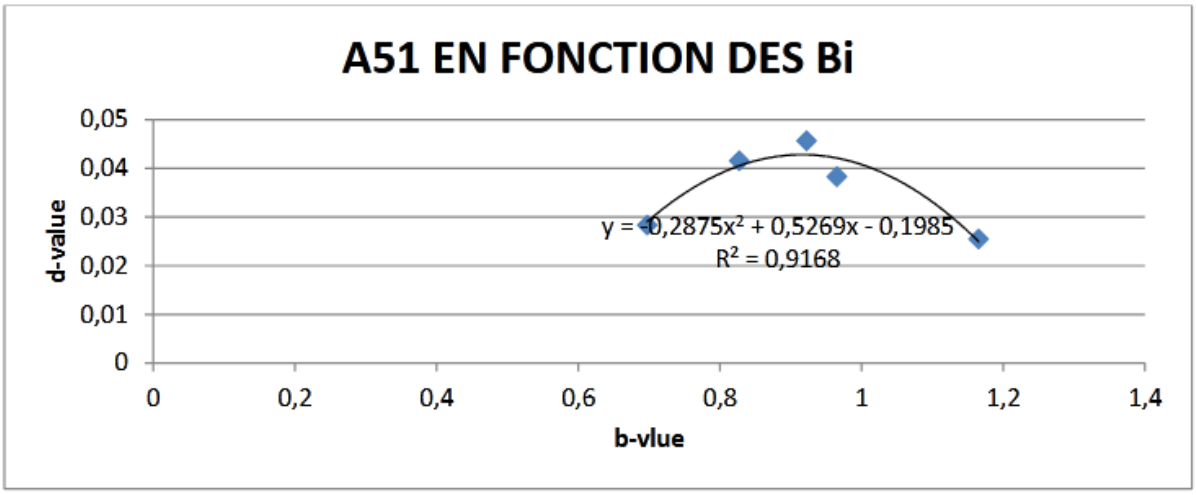

Figure 13 a: Correlation between the b-value and the d-value for zone A51T according to horizontal subdivisions

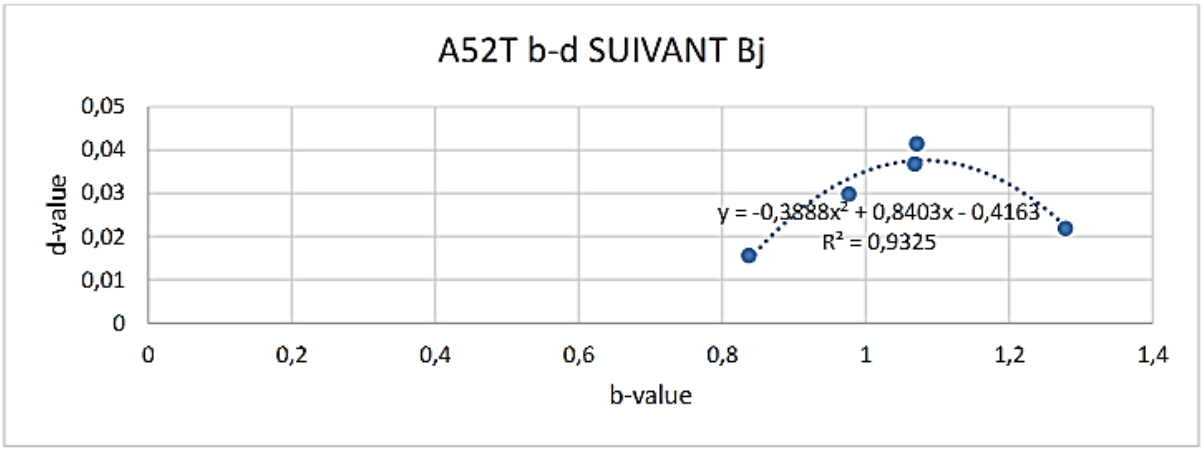

Figure 13 b: Correlation between the b-value and the d-value for zone A52T according to horizontal subdivisions

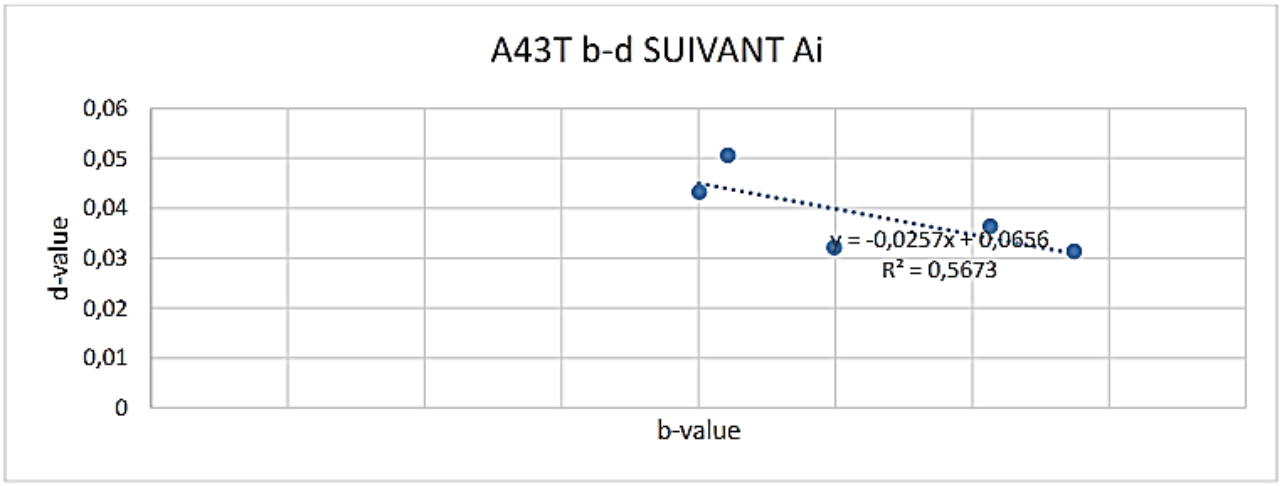

Figure 13c: Correlation between the b-value and the d-value for the A43T zone according to vertical subdivisions

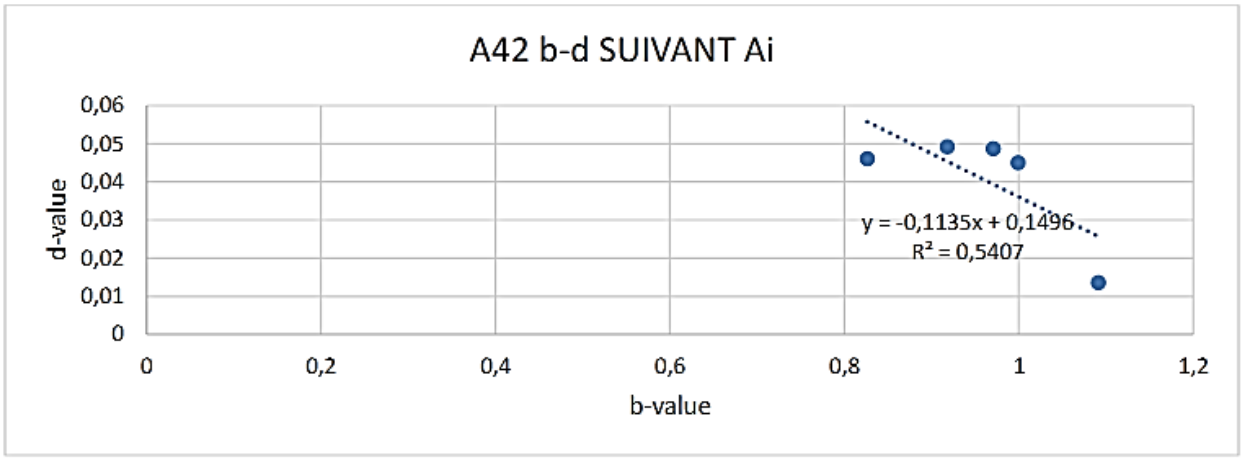

Figure 13 d: Linear correlation between the b-value and the d-value for the A43T zone according to vertical subdivisions

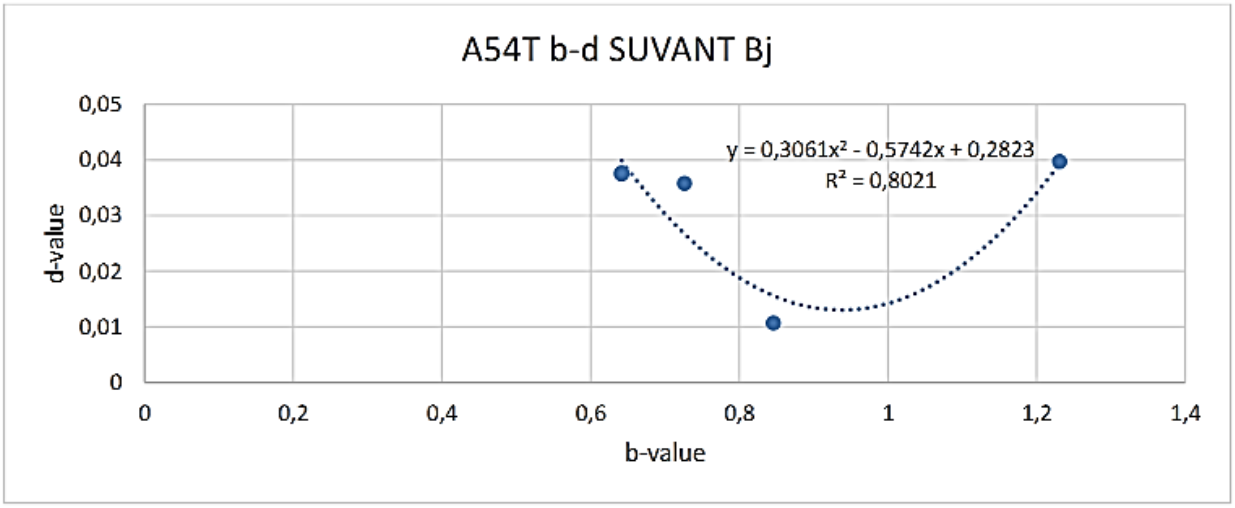

Figure 13e: Correlation between b-value and d-value for zone A54T based on horizontal subdivisions

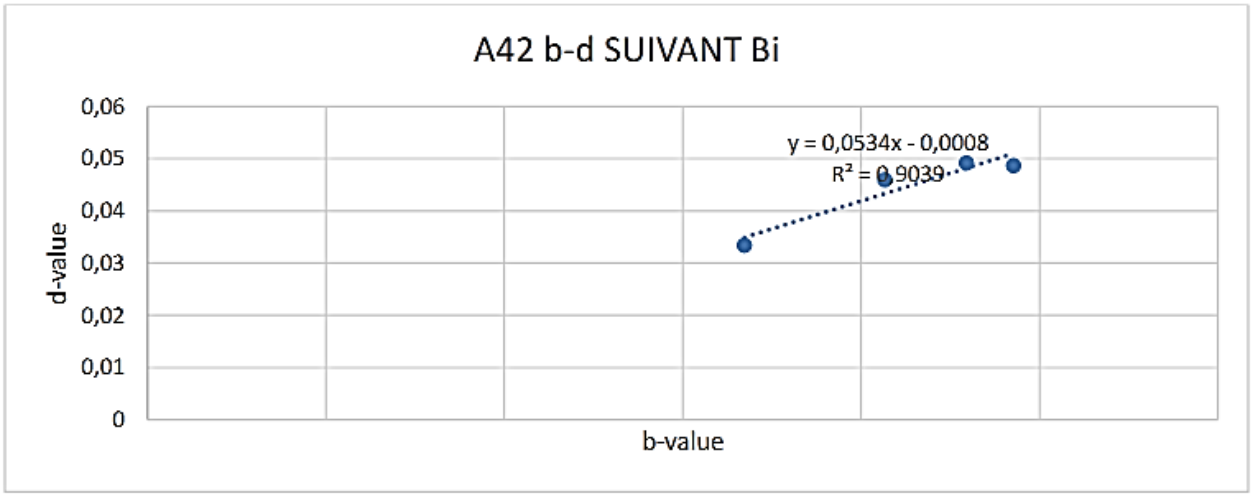

Figure 13f: Linear correlation between the b-value and the d-value for the A42T zone according to the horizontal subdivisions

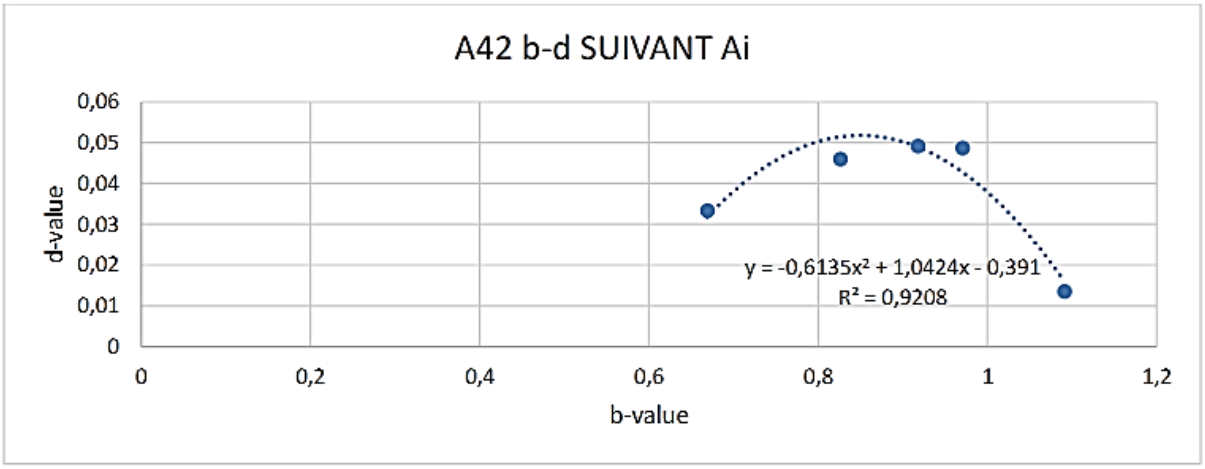

Figure 13g: Correlation between the b-value and the d-value for the A42T zone according to vertical subdivisions

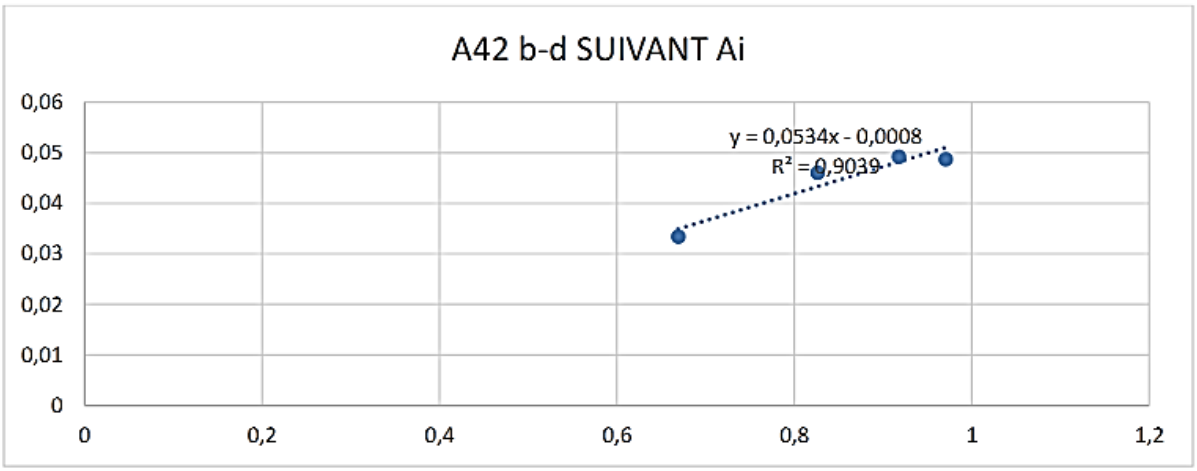

Figure 13h: Linear correlation between the b-value and the d-value for zone 42T according to horizontal subdivisions

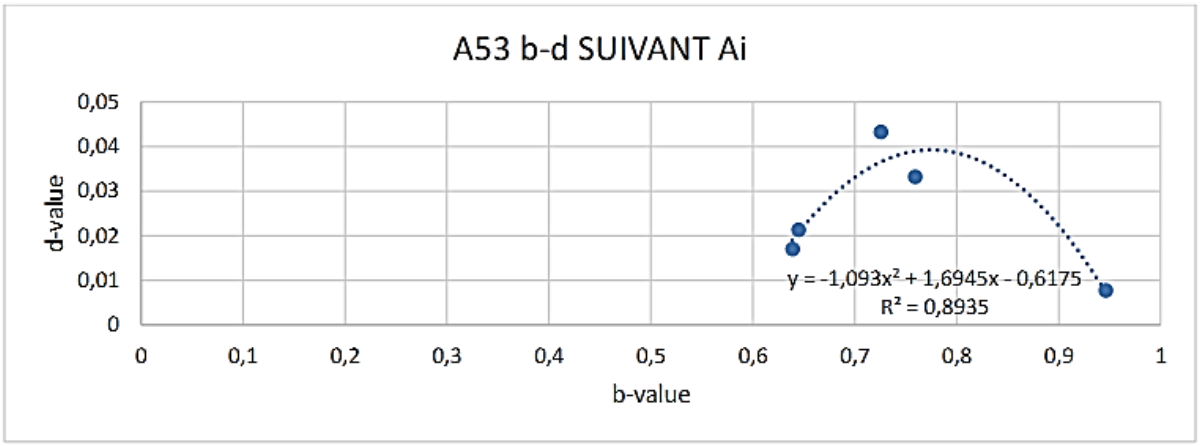

Figure 13i: Correlation between the b-value and the d-value for the A53T zone according to vertical subdivisions

Observation of the shapes of these curves reveals two large families, one consisting of linear curves, the other of parabolic curves (Table 23)

Table 23: classification of zones according to the shape of the correlation curves

	curve		RIGHT	
Shape of curves	Positive concavity	Negative concavity	Positive slope	Negative slope
Affected areas	A54T following Ai	A51T next Bj A52T next Bj A53T next Bj A42T following Ai	A42 following Ai A42T next Bj	A43T following Ai A42T following Ai

Analysis of the results in this table highlights the following facts:

- The zones located between 25 and 30°E, in the Congolese rift (A42, A43 and A44) have a linear shape
- Those located between 30 and 35°E, in the Malawi-Zambezi rift (A51, A52, A53 and A54) have a parabolic shape,
- However, zones A42T (Kivu zone) and A54T (Malawi zone) have nuanced trends (exceptions), therefore straddling the two previous groups.

3.3. Location of main faults

The location of underground faults is often done by exploiting the gravity and geomagnetic data of the region (Mbata, 2023; Ngindu, 2021; Mulopo, 2023; Tondozi, 2018). As far as we are concerned, the interest is focused on the location of said faults by exploiting the fundamental data of seismic activity.

To do this, this location will be based on the hypothesis that: “the main underground faults are located in places where the seismic activity module is at its peak”. This paroxysm corresponds in figure (7) to the zone where the modulus is the highest; which gives rise to the results contained in Figures (14-15) for zones A42 and A43.

AREAS	A1 (25-26°E)	A2 (26-27°E)	A3 (27-28°E)	A4 (28-29°E)	A5 (29-30°E)
A42 (25-30°E, 6-1°N) AREA VIRUNGA-KIVU					
A43 (25-30°E, 1°N-4°S) AREA TANGANYIKA-KIVU					

Figure 14: Location of main and minor faults in the Aij zone

Reading Figure (14) responds to the legend above:

- Red color: the main fault is located in layer G (0-10 km)
- Yellow color: the main fault is located in layer C (10-20 km),
- Green color: the main fault is located in layer C' (20-40 km),
- Blue color: the main fault is located in layer C'' (>40 km),
- Purple color: the main fault is located in the C' and C'' layer, therefore (>20 km),
- White color: no main fault, but minor faults can be found.

The comparative analysis of these results reveals the following:

- For both zone A42 and zone A43, no main fault was observed in zone A4; this zone is therefore the most stable.
- While the position of the main faults at layer G (0-10 km) is located at A5 for seismic zone A42, these faults are located at zone A3 for A43 for the same layer (G) and the opposite at the layer C (10-20 km); this observation could be explained by:

    - ❖ The heterogeneity of the soil above 20 km,
    - ❖ The position of two zones: zone A42, including Lake Kivu, is located at a height of 1462 km and a depth of 485 km. The A43 zone, including Lake Tanganyika, is located at a height of 780 km and a depth of 1433 km,
    - ❖ The orientation of the faults in these two zones are opposite (Figure 1,2 and 9): NW-SE orientation for Lake Tanganyika (Bopili, 2009) and NE-SW for Lake Kivu .

We note a sort of alternation or compensation in the geodynamics between the two zones
towards regions close to the rift at a depth not exceeding 20 km,

Beyond twenty kilometers in depth, the main faults are almost, for both A42 and A43, located on A1; which means that :

- ❖ From the surface to a depth of 20 km, the faults are close to the rift, moving away from it beyond the depth of 20 km (position of the Conrad discontinuity),
- ❖ The soil structure is more homogeneous and denser beyond 20 km than above, in accordance with the literature ( ),

In short, we conclude by saying that the characterization scale designed is reasonable and that the hypothesis put forward is also valid.

4. GENERAL CONCLUSION AND OUTLOOK

This research aims to highlight the fine structure of the seismic zones of the western branch of the East African rift system using the unified scale of characterization and the location of the main faults, leading to the following conclusions:

Regarding the fine structure, we note:

- Statistics on seismic species discovered in the region show:

    - ❖ In total, we identified 89 seismic species,
    - ❖ There are 28 (42%) seismic species common to all areas,
    - ❖ There are 17% of species exclusive to zones A51, A52, A52 and A54, zones between 20 and 25°E,
    - ❖ There are 17% of seismic species exclusive to zone A42 subdivided into depth zones (A42G, A42B, A42B', A42B'', A42C, A42C', A42C'') in the table (),
    - ❖ There are 17% of species exclusive to zone A42 subdivided into depth zones (A42G, A42B, A42B', A42B'', A42C, A42C', A42C'').
    - ❖ The average conservation rate of species is 5%. We conclude that species are rarely preserved by going deep,

- Generally speaking, all of these 21 zones align, depending on the color arrangements, on one of two shapes:
    - ❖ A symmetrical shape, these are A51T, A52T, A52T and A54T, therefore the zones located between 20° and 25°E,
    - ❖ A bipolar form (two groups of colors) for all areas located between 25° and 20°E; these are the A42T, A42T, A44T and their derivatives.

- From these curves comparing the rate of resemblance to that of resemblance, the following observations emerge:
    - ❖ With a few exceptions, there is a correlation between the absolute resemblance rate and the relative resemblance rate;
    - ❖ With a few exceptions, except at A42G and A42B in the Virunga-Kivu region, there is a correlation between the absolute or relative rate of resemblance and the rate of heterogeneity,
    - ❖ There is a correlation between the number of curves and the rate of heterogeneity; in fact, we see that the number of curves decreases with the rate of heterogeneity: at less than 50% of this rate, we have fewer than three structural curves.
    - ❖ The average rate of heterogeneity is 49%, it is on average higher (55%) between 30 and 35°E and less between 25 and 30°E,
    - ❖ the combination of the three parameters (rate of resemblance, heterogeneity and conservation of the species) brings together

85% of the structures in the same class, the A42T zone (Virunga-Lake Kivu zone) being an exception and partially the Tanganyika zone (A43B'),
- ❖ We observe that the structure of the A44 zone (Upemba rift zone, upper Katanga region) straddles A42T (Virunga-Lake Kivu zone) and A43T (Tanganyika zone), with implication on the orientation failures ,
- ❖ There is reason to affirm that the structure of the entire DRC is determined or predominated by that of the A42B" zone (Virunga zone at a depth exceeding 30km).

- The analysis of the results based on the b-alue and the d-value, one measuring seismic activity, the other the soil structure, indicates that:
  - ❖ The zones located between 25 and 30°E, in the Congolese rift (A42, A43 and A44) have a linear shape with some particularities each,
  - ❖ Those located between 30 and 35°E, in the Malawi-Zambezi rift (A51, A52, A53 and A54) have a parabolic shape,
  - ❖ However, zones A42T (Kivu zone) and A54T (Malawi zone) have trends
  - ❖ The resemblance rate, based on structural factors, between these two zones is 25%
  - ❖ The first zone is less seismic than the second, one having a form factor (III), the other (IV)
  - ❖ Each of these seven zones, whose heterogeneity rate was 38% (Figure 2), no longer resembles itself alone; therefore the heterogeneity rate increases to 100%

The location of the main faults is based on the hypothesis that: “the main faults are located in places where the module of seismic activity is at its peak”. The exploitation of this hypothesis and the structure curves have:

- Made it possible to locate the main and secondary faults,
- Shown that going deeper, these faults change position; the shape is no longer vertical nor rectilinear, but wavy and serpentine,
- Showed that these results are in accordance with field observations and literature
- allowed us to note that from the surface to a depth of 20 km, the faults of the Kivu (A42) and Tanganyika (A43) zones are located near the rift, to move away from it beyond the depth of 20 km (corresponding to the average position of the Conrad discontinuity),
- While the position of the main faults at layer G (0-10 km) is located at A5 for seismic zone A42, these faults are located at zone A3 for A43 for the same layer (G) and the opposite at the layer C (10-20 km) and are all located at A1 beyond 20 km,

In short, we say that our model based on the discovery of seismic species and the generation of the characterization scale is reasonable and that the hypothesis put forward is valid. Indeed, their exploitation has allowed a better characterization, both quantitative and qualitative, of the soil structure and its geodynamics using fundamental seismic parameters. These results go beyond what is known.

REFERENCES

1. Bantidi M., Wafula M., Mavambou, Mukange B., Zana Nd., (2014a). Probabilistic assessment of seismic hazard in Lake Tanganyika Rift accounting for local geologies conditions. 2015. *International Journal of Geology, Agriculture and Environmental Sciences*. Vol.03 Issue 02 (April 2015), pp24-29.

2. Bantidi M., Mukange B., et Zana N., (2014b). Structure de la sismicité de la Branche occidentale des Rifts Valleys du système des Rifts Est-africains ; de 1954 à 2010, *International Journal of Innovation and Applied Studies*, ISSN 2028-9324 Vol. 9 No. 4 Dec. 2014, pp.1562-1581.

3. Biliki K;. and al.,(2021). Interpretation of Gravity Data and Contribution to the Study of the Geological Structure of the Province of Mai-Ndombe in DR. Congo: Implications in the Exploration of Hydrocarbons. International Journal of Innovative Science and Research Technology, Volume 6, Issue 4, April – 2021, pp213-921.

4. Borden J-P., (1988). *Biologie-Géologie*. Première S. Paris: Bordas

5. Bopili M.L., (2009). *Etudes des fluctuations de la température et de la vitesse des vents au lac Tanganyika (une analyse par ondelettes).* Thèse de doctorat : Université de Kinshasa, Faculté des Sciences, Département de Physique. pp. 9-28

6. Lay T., and Wallace T., (1995). *Modern Global seismology*. New-York : Academic Press

7. Mavonga Tuluka G., (2009).*Seismic hazard assessment and volcanogenic seismicity for the Democratic Republic of Congo and surrounding areas, western Rift valley of Africa*. Thèse de Doctorat: University of the Witwatersrand (Johannesburg), Faculty of Sciences.

8. Mbata A. and al., (2023). A comparative structural study of Southern region shallow basement of the North-Kivu Province (DR. Congo) by gravity and magnetic data analysis. Journal of Geoscience and environnement protection, Vol 11, pp 90-117.https:// doi.org/10.4236/gep.2023.119007.

9. Mukange B., Bantidi M., Zana Nd., (2013). Structure de la sismicité de la Branche orientale des Rifts Valleys du système des Rifts Est-africains ; de 1954 à 2010. *Revue Congolaise des Sciences Nucléaires.* vol.27, pp 151-169.

10. Mukange B., Bantidi M., Zana L., Wafula M., Zana Nd., (2015). The isoseismal map and their implication to underlining ground degree of heterogeneity (Kabalo quake's case, September 11, 1992, magnitude 6.7, Upemba Rift). *Greener Journal of Geology and Earth Sciences*, vol. 3 (2), pp 030-042.

11. Mukange B., (2016). *Conception d'un modèle physique pour la caractérisation et la surveillance de l'activité sismique et son implication géologique (Cas de la République Démocratique du Congo).* Thèse de Doctorat : Université de Kinshasa, Faculté des Sciences. Département de Physique.

12. Mukange Besa, (2021). *Cours de Géophysique générale*. Université de Kinshasa, Faculté des Sciences.

13. Mukange B., (2021a). Design of a unified scale for the characterization of seismic activity. International Journal of Innovative Science and Research Technology, Volume 6, Issue 7 , July– 2021, pp.1407-1422. www.ijisrt.com

14. Mukange B., (2021b). Application of the unified scale to the characterization of seismic activity of the Democratic Republic of Congo and its surroundings (comparative study for Africa, Indonesia and the Pacific coast of Central America). International Journal of Innovative Science and Research Technology, Volume 6, Issue 7, July– 2021, pp.1516-1555. www.ijisrt.com

15. Mukange B., (2023a). Characterization of the volcano-seismic activity around Nyiragongo volcano and location of its crater by means of unified scale. *Greener Journal of Geology and Earth Sciences*, 5(1) December 2023: 28-51. http//gjournals.org/GJGES.

16. Mukange B., (2023b). Characterization of the volcano-seismic activity around Nyamulagira volcano and location of its crater by means of unified scale. *Greener Journal of Geology and Earth Sciences*, 5(1) December 2023: 52-75. http//gjournals.org/GJGES.

17. Mulopo, (2023). *Analyse des corrélations entre les linéaments et les accidents tectoniques de la région de Lubumbashi-Kipushi : contribution à l'étude classique de la tectonique régionale en République Démocratique du Congo*. Thèse de Doctorat : Université Pédagogique Nationale, Faculté des Sciences. Département de Physique

18. Musitu M. and al., (2023). Structural mapping of Kakobola and its surroundings by analyzing geomagnetic data. Journal of Geoscience and environnement protection, Vol 11, pp 64-89.https:// doi.org/10.4236/gep.2023.119006.

19. Ngindu D. and al., (2021). New Faults from the Geodynamics of South Katanga in D.R.Congo. International Journal of Innovative Science and Research Technology, Vol(6) Issue 1(January 2021),pp1596-1689.

20. Tondozi K. and al, (2018). Interpretation of gravity anomalies maps and contribution to the structural study of a sedimentary basin of major petroleum interest: Case of the Busira sub-basin in the Central basin of the DR Congo, IJIAS Vol. 24 N°1, p. 68-88.

Cite this Article: Mukange, BA; Katwika, C; Jalum, B; Zana, NA; Tondozi, KF (2023). Highlighting the Fine Structure of the Seismic Zones of the Western Branch of the East African Rift System Using the Unified Characterization Scale and Its Geological Implication. *Greener Journal of Geology and Earth Sciences*, 5(1): 76-108.